



# Stability of the Dynamical Motion of a Damped 3DOF Auto-parametric Pendulum System

T. S. Amer<sup>1</sup> · M. A. Bek<sup>2</sup> · M. S. Nael<sup>2</sup> · Magdy A. Sirwah<sup>1</sup> · A. Arab<sup>2</sup>

Received: 25 October 2021 / Revised: 5 March 2022 / Accepted: 27 March 2022 / Published online: 21 April 2022  
© The Author(s) 2022

## Abstract

**Purpose** The motion of three degrees-of-freedom (DOF) of an automatic parametric pendulum attached with a damped system has been investigated. The kinematics equations of this system have been derived employing Lagrange's equations in accordance to it's the generalized coordinates.

**Methods** The method of multiple scales (MMS) has been used to obtain the solutions of the controlling equations up to the third-order of approximation. The solvability criteria and modulation equations for primary external resonance have been explored simultaneously.

**Results** The non-linear stability approach has been used to analyze the stability of the considered system according to its different parameters. Time histories of the amplitudes and the phases of this system have been graphed to characterize the motion of the system at any given occurrence.

**Conclusions** The different zones of stability and instability of this study have been checked and examined, in which the system's behavior has been revealed to be stable for various values of its variables.

**Keywords** Non-linear vibrations · Resonance · Auto-parametric vibration · Perturbation techniques

## Introduction

The development of vibrating systems is seen as one of the critical developments in mechanics, because of its different applications for the duration of regular daily existence, for example, building structures, rotor dynamics, rotor components, pumps, sieves, the motion of ships, compressors, and transportation devices [1–3].

Auto-parametric system is one of the essential systems that at least consists of two non-linearly subsystems. The first can be excited by an external harmonic force attached to a second one called an absorber. In this manner, one can get the essential parametric resonance of other subsystems (auto-parametric interaction) by decreasing the reaction of the first one [4–10]. The non-linear damping response 2DOF dynamical system connected with spring is investigated in [7]. In [8], the authors studied a dynamical oscillatory system with 4DOF comprising an auto-parametric pendulum and attached to a rigid body. Nonetheless, the auto-parametric system's behavior under the effect of kinematic excitation is studied numerically and illustrated experimentally in [9]. The authors examined whether the motion was regular or not through specific plots. In [10], the authors investigated an auto-parametric system's behavior consisting of a pendulum absorber connected to a damped vibrated system. The resonance case is obtained by using the technique for harmonic balance [5]. The MMS is utilized in [11] to acquire the auto-parametric states of a damped Duffing system linked with a pendulum. By uprightness of this method, a two coupled mass spring response is gotten in [12]. The author explained new excitation conditions within the sight of auto-parametric resonance. This resonance of an oscillatory system in the existence

✉ T. S. Amer  
tarek.saleh@science.tanta.edu.eg

M. A. Bek  
m.ali@f-eng.tanta.edu.eg

M. S. Nael  
mohamed.nail@f-eng.tanta.edu.eg

Magdy A. Sirwah  
magdy.sirwah@science.tanta.edu.eg

A. Arab  
asmaa\_arab@f-eng.tanta.edu.eg

<sup>1</sup> Mathematics Department, Faculty of Science, Tanta University, Tanta 31527, Egypt

<sup>2</sup> Physics and Engineering Mathematics Department, Faculty of Engineering, Tanta University, Tanta 31734, Egypt

of a non-linear coupling term of third-order is discussed in [13]. The stability and the system's bifurcation under external harmonic forces are explored [14, 15]. Besides, the MMS is used to get an autonomous framework up to the third order for a spring-suspended motion on a circular path [16]. The response of 2DOF for a non-linear dynamical system characterized by a damped elastic pendulum in an inviscid fluid flow is examined in [17]. The fourth-order Runge–Kutta calculation of the ode45 solver [18] is utilized in [19] to get the numerical solution of the state of an oscillatory rigid body using the Matlab program. The author showed the achieved results, which are consistent with the previous works. The harmonic damped spring pendulum's behavior is explored in [20] when the hanged point follows an elliptic route with stationary angular velocity. The MMS is used to obtain resonance cases and get the modulation equation that decides all possible steady-state solutions. The impersonalized of this model is introduced in [21] where a rigid body is attached to a spring in the existence of a harmonic force along the spring's arm adding two moments, the first at the point of the body with the spring and the second at the auto-parametric pendulum suspending point of the pendulum. The resonances cases are explored and the solvability conditions are studied. The comparison between both the numerical solutions and approximate ones explain the high consistency between them.

Then the vibrational systems must be controlled in our applications through absorbers' existence to avoid disturbance and devastation of the structures or the studied systems. There are a lot of works studied such motions, for example [20–25]. Recently, the movement of a damped pendulum's of rigid body with 3DOF is explored in [26] and [27] for the cases of linear and non-linear Stiffness, respectively. In [24], the authors researched a dynamical system consisting of a pendulum and absorber along the pendulum arm. The system is exposed to an active control, for example, the velocity with a negative value and angular displacement or the squares or cubic values. The approximate solutions are obtained using the MMS. The influences of absorbers on the system's behavior and the stability of the system and are considered. The response of non-linear spring pendulum 2DOF is studied in [25] at different resonance cases and in the presence of control.

In this work, the 3DOF dynamical motion of an auto-parametric system consists of mass  $M$  connected with two massless springs with linear stiffness is investigated. The studied motion is examined under the influence of external harmonic forces. The equations of motion (EOM) are investigated applying Lagrange's equations. The MMS is used to obtain the equations' solutions up to the third approximation and discuss the system's resonance cases. Also, the phase and amplitude variables are discussed to investigate these solutions at the steady-state in line with the stability requirements. The domain of stability and instability areas is studied and analyzed. The variations of the obtained solutions are plotted for different parameters to show the influence of the applied external forces and moments on the behavior of the system under consideration.

## Problem Formulation

Let us consider a dynamic system consisting of a mass  $M^*$  connected to two massless springs of stiffness  $k_1$  and  $k_2$  with linear stiffness  $k_1 r$  and  $k_2 x$  respectively. These springs are attached with linear damper with damping coefficients  $c_1$ ,  $c_2$ , and  $c_3$ . It worthy to mention that, the first spring is a pendulum with length  $\ell$  and the other one is horizontally directed with length  $\ell'$  as shown in Fig. 1. Consider a moment  $M(t) = M_0 \cos(\varpi_3 t)$  that acts at the point  $z$  besides two external harmonic forces; the first one  $F_r(t) = F_1 \cos(\varpi_1 t)$  acts on the mass  $m$  along the pendulum arm and the other one is  $F_x(t) = F_2 \cos(\varpi_2 t)$  acts on the horizontal direction of  $X$ -axis in which  $\varpi_1$ ,  $\varpi_2$ , and  $\varpi_3$  are the frequencies of the external forces and moment. Therefore, the motion of the mechanical system can be described by the generalized coordinates  $x(t)$  (translation  $M$ ),  $r(t)$  (elongation of the spring pendulum), and  $\theta(t)$  (link rotation).

Let  $L = T - V$  indicates Lagrangian, where  $T$  and  $V$  represent kinetic and potential energies of the considered system that have the forms

$$T = \frac{1}{2}(m \dot{r}^2 + 2m \sin \theta \dot{r} \dot{x} + (m + M^*) \dot{x}^2 + 2m \cos \theta (\ell + r) \dot{\theta} + m(\ell + r)^2 \dot{\theta}^2) \quad (1)$$

$$V = \frac{1}{2}k_1 r^2 + \frac{1}{2}k_2 x^2 + mg(\ell + r)(1 - \cos \theta),$$

where  $g$  is the acceleration of gravity and dots denote to the time differentiation of the variables  $r$ ,  $x$ , and  $\theta$ .

It is known that the potential energy  $V$  is the sum of the energies due to the elongation of the two springs and the gravitational force of the connector. Consequently, Lagrange's equations have in the form

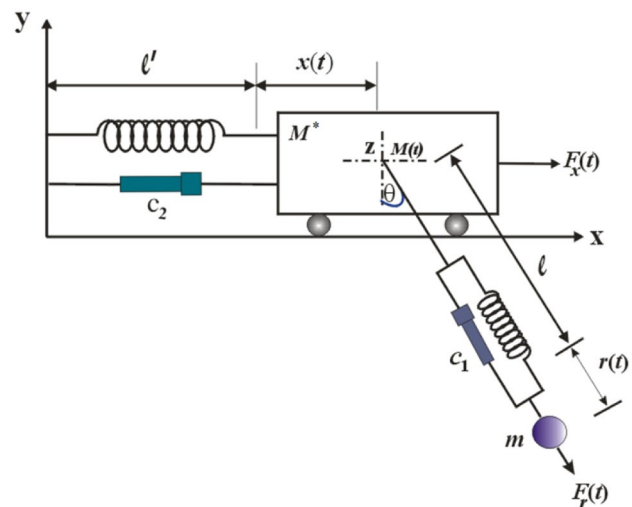


Fig. 1 Description of the auto-parametric system

$$\begin{aligned} \frac{d}{dt} \left( \frac{\partial L}{\partial \dot{r}} \right) - \left( \frac{\partial L}{\partial r} \right) &= F_1 \cos(\varpi_1 t) - c_1 \dot{r}, \\ \frac{d}{dt} \left( \frac{\partial L}{\partial \dot{x}} \right) - \left( \frac{\partial L}{\partial x} \right) &= F_2 \cos(\varpi_2 t) - c_2 \dot{x}, \\ \frac{d}{dt} \left( \frac{\partial L}{\partial \dot{\theta}} \right) - \left( \frac{\partial L}{\partial \theta} \right) &= M_0 \cos(\varpi_3 t) - c_3 \dot{\theta}. \end{aligned} \tag{2}$$

Here  $(\dot{r}, \dot{x}, \dot{\theta})$  refer to the generalized velocities. Substituting (1) into (2), we get the EOM as follows:

$$\begin{aligned} m \ddot{r} + k_1 r &= mg \left( 1 - \frac{\theta^2}{2} \right) + m r \dot{\theta}^2 - mg + m \ell \dot{\theta}^2 \\ -m \ddot{x} \left( \theta - \frac{\theta^3}{6} \right) - c_1 \dot{r} + F_1 \cos(\varpi_1 t), \end{aligned} \tag{3}$$

$$\begin{aligned} (m + M^*) \ddot{x} + k_2 x &= m(\ell + r) \left( \theta - \frac{\theta^3}{6} \right) \dot{\theta}^2 - m \ddot{r} \left( \theta - \frac{\theta^3}{6} \right) \\ -2m \dot{r} \dot{\theta} \left( 1 - \frac{\theta^2}{2} \right) \\ -m \left( 1 - \frac{\theta^2}{2} \right) (\ell + r) \ddot{\theta} - c_2 \dot{x} + F_2 \cos(\varpi_2 t), \end{aligned} \tag{4}$$

$$\begin{aligned} m \ell^2 \ddot{\theta} + mg(\ell + r) \left( \theta - \frac{\theta^3}{6} \right) &= -2m \ell r \ddot{\theta} - m \ell \ddot{x} \left( 1 - \frac{\theta^2}{2} \right) - m r (\ell + r) \\ -2m \ell \dot{r} \dot{\theta} - 2m r \dot{r} \dot{\theta} - m r \ddot{x} \left( 1 - \frac{\theta^2}{2} \right) - c_3 \dot{\theta} + M_0 \cos(\varpi_3 t). \end{aligned} \tag{5}$$

It is obvious that the last three equations represent second-order non-linear differential equations in terms of  $r, x$ , and  $\theta$ .

Considering the following dimensionless variables

$$\begin{aligned} \frac{r}{\ell} = \varepsilon \tilde{r}, \quad \frac{x}{\ell} = \varepsilon \tilde{x}, \quad \theta = \varepsilon \tilde{\theta}, \quad t = \sqrt{\frac{\ell}{g}} \tilde{t}, \quad \frac{F_1}{mg} = \varepsilon^3 \tilde{f}_1, \quad \frac{h}{\ell} = \varepsilon I, \quad \omega_1^2 = \frac{k_1}{m}, \\ \omega_2^2 = \frac{\ell}{g}, \quad W_1 = \frac{\varpi_1}{\omega_2}, \quad W_2 = \frac{\varpi_2}{\omega_2}, \quad W_3 = \frac{\varpi_3}{\omega_2}, \quad \frac{c_1}{m} \sqrt{\frac{\ell}{g}} = \varepsilon^2 \tilde{c}_1, \\ \frac{c_2}{(m + M^*)} \sqrt{\ell g} = \varepsilon^2 \tilde{c}_2, \quad \frac{F_2}{(m + M^*)g} = \varepsilon^3 \tilde{f}_2, \quad B = \mu g \ell, \quad \frac{g \ell}{B} = \varepsilon J, \quad \Omega_1^2 = \omega_1^2 \omega_2^2, \\ \frac{c_3}{m} \sqrt{\frac{2}{3g}} = \varepsilon^2 \tilde{c}_3, \quad \mu = \frac{m}{m + M^*}, \quad \frac{M_0}{m g \ell} = \varepsilon^3 \tilde{f}_3, \quad h = m \ell^2 g, \quad \Omega_2^2 = \frac{k_2 \ell}{(m + M^*)g}, \end{aligned} \tag{6}$$

to convert (3–5) into the following dimensionless form:

$$\begin{aligned} \varepsilon \ddot{\tilde{r}} + \Omega_1^2 \varepsilon \tilde{r} &= -\varepsilon^2 \left( \frac{\tilde{\theta}^2}{2!} - \dot{\tilde{\theta}}^2 + \tilde{x} \tilde{\theta} + \tilde{c}_1 \tilde{r} \right) + \varepsilon^3 [\tilde{r} \dot{\tilde{\theta}}^2 + \tilde{f}_1 \cos(W_1 \tilde{t})], \\ \varepsilon \ddot{\tilde{x}} + \Omega_2^2 \varepsilon \tilde{x} &= \mu \varepsilon^3 \tilde{\theta}^2 \theta - \mu \varepsilon^2 \tilde{r} \theta - \varepsilon^2 J \ddot{\tilde{\theta}} (1 + \varepsilon \tilde{r}) - \varepsilon^2 \tilde{c}_2 \dot{\tilde{x}} - 2\mu \varepsilon^2 \tilde{r} \dot{\tilde{\theta}} + \varepsilon^3 \tilde{f}_2 \cos(W_2 \tilde{t}), \\ \varepsilon \ddot{\tilde{\theta}} + \varepsilon \tilde{\theta} &= -\varepsilon^2 \tilde{r} \tilde{\theta} + \varepsilon^2 \tilde{r} \dot{\tilde{\theta}} - \varepsilon^2 I \ddot{\tilde{x}} (1 - \varepsilon^2 \frac{\tilde{\theta}^2}{2!}) - 2\varepsilon^2 \tilde{r} \dot{\tilde{\theta}} - 2\varepsilon^3 \tilde{r} \tilde{r} \dot{\tilde{\theta}} - \varepsilon^2 r \ddot{\tilde{x}} (1 - \varepsilon^2 \frac{\tilde{\theta}^2}{2!}) \\ &\quad - \varepsilon^2 \tilde{r} (1 + \varepsilon \tilde{r}) \ddot{\tilde{\theta}} - \varepsilon^2 \tilde{c}_3 \dot{\tilde{\theta}} + \varepsilon^3 \tilde{f}_3 \cos(W_3 \tilde{t}). \end{aligned} \tag{7}$$

Here,  $\varepsilon$  is known as the small parameter affecting the coupling between the pendulum absorber and the damping, external force, and nonlinearities of the system. Its important influence appears in current non-linear frequency analysis at the desired approximation. To simplify the notation, the sign  $\sim$  (tilde) is omitted below.

### The Proposed Method

The MMS is an analytical method that used to determine approximate solutions with high accuracy of non-linear differential equations for which exact solutions cannot be obtained. It can be used to demonstrate, predict and describe phenomena in vibrating systems that caused by non-linear effects. Moreover, it can be applied to non-linear and linear systems with variable coefficients or complex boundary conditions, where the exact closed-form solution is unknown. Therefore, this method is utilized to solve the system of Eqs. (7) up to the third approximation. Therefore, we need three timescales, which has the forms  $T_n = \varepsilon^n T (n = 0, 1, 2)$  where  $T_0, T_1$ , and  $T_2$  are various time scales. According to the method of the MS perturbation, the solutions  $r, x$ , and  $\theta$  can be sought in the powers of  $\varepsilon$  as [28, 29]

$$\begin{aligned} r &= \sum_{k=1}^3 \varepsilon^k r_k(T_0, T_1, T_2) + O(\varepsilon^4), \\ x &= \sum_{k=1}^3 \varepsilon^k x_k(T_0, T_1, T_2) + O(\varepsilon^4), \\ \theta &= \sum_{k=1}^3 \varepsilon^k \theta_k(T_0, T_1, T_2) + O(\varepsilon^4). \end{aligned} \tag{8}$$

The derivatives in terms of the new time scales in (8) are expressed as follows [5]:

$$\begin{aligned} \frac{d}{dT} &= \frac{\partial}{\partial T_0} + \varepsilon \frac{\partial}{\partial T_1} + \varepsilon^2 \frac{\partial}{\partial T_2}, \\ \frac{d^2}{dT^2} &= \frac{\partial^2}{\partial T_0^2} + 2\varepsilon \frac{\partial^2}{\partial T_0 \partial T_1} + \varepsilon^2 \left( \frac{\partial^2}{\partial T_1^2} + 2 \frac{\partial^2}{\partial T_0 \partial T_2} \right) + O(\varepsilon^3). \end{aligned} \tag{9}$$

Substituting (8) and (9) into (7) and collecting the coefficients of equal powers of  $\varepsilon$  in both sides leads to the following system containing the following nine partial differential equations.

**Order ( $\varepsilon$ )**

$$\frac{\partial^2 r_1}{\partial T_0^2} + \Omega_1^2 r_1 = 0, \tag{10}$$

$$\frac{\partial^2 x_1}{\partial T_0^2} + \Omega_2^2 x_1 = 0, \tag{11}$$

$$\frac{\partial^2 \theta_1}{\partial T_0^2} + \theta_1 = 0. \tag{12}$$

**Order of ( $\varepsilon^2$ )**

$$\frac{\partial^2 r_2}{\partial T_0^2} + \Omega_1^2 r_2 = -2 \frac{\partial^2 r_1}{\partial T_0 \partial T_1} - \frac{1}{2} \theta_1^2 + \left( \frac{\partial \theta_1}{\partial T_0} \right)^2 - \frac{\partial^2 x_1}{\partial T_0^2} \theta_1, \tag{13}$$

$$\frac{\partial^2 x_2}{\partial T_0^2} + \Omega_2^2 x_2 = -2 \frac{\partial^2 x_1}{\partial T_0 \partial T_1} - \mu \frac{\partial^2 r_1}{\partial T_0^2} \theta_1 - J \frac{\partial^2 \theta_1}{\partial T_0^2} - 2\mu \frac{\partial r_1}{\partial T_0} \frac{\partial \theta_1}{\partial T_0}, \tag{14}$$

$$\frac{\partial^2 \theta_2}{\partial T_0^2} + \theta_2 = -2 \frac{\partial^2 \theta_1}{\partial T_0 \partial T_1} - r_1 \theta_1 + r_1 \frac{\partial^2 \theta_1}{\partial T_0^2} - I \frac{\partial^2 x_1}{\partial T_0^2} - 2 \frac{\partial^2 r_1}{\partial T_0^2} \frac{\partial^2 \theta_1}{\partial T_0^2} - r_1 \frac{\partial^2 \theta_1}{\partial T_0^2}, \tag{15}$$

**Order of ( $\varepsilon^3$ )**

$$\begin{aligned} \frac{\partial^2 r_3}{\partial T_0^2} + \Omega_1^2 r_3 &= -\frac{\partial^2 r_1}{\partial T_1^2} - 2 \frac{\partial^2 r_1}{\partial T_0 \partial T_1} - 2 \frac{\partial^2 r_2}{\partial T_0 \partial T_1} - \theta_1 \theta_2 + r_1 \left( \frac{\partial \theta_1}{\partial T_0} \right)^2 - \frac{\partial^2 x_1}{\partial T_0^2} \theta_2 \\ &+ 2 \frac{\partial \theta_1}{\partial T_0} \frac{\partial \theta_1}{\partial T_1} - 2 \frac{\partial^2 x_1}{\partial T_0 \partial T_1} \theta_1 + \frac{\partial^2 x_2}{\partial T_0^2} \theta_1 - c_1 \frac{\partial r_1}{\partial T_0} + f_1 \cos(W_1 T_0), \end{aligned} \tag{16}$$

$$\begin{aligned} \frac{\partial^2 x_3}{\partial T_0^2} + \Omega_2^2 x_3 &= -\frac{\partial^2 x_1}{\partial T_1^2} - 2 \frac{\partial^2 x_1}{\partial T_0 \partial T_1} - 2 \frac{\partial^2 x_2}{\partial T_0 \partial T_1} + \mu \left( \frac{\partial \theta_1}{\partial T_0} \right)^2 \theta_1 - \mu \frac{\partial^2 r_1}{\partial T_0^2} \theta_2 - 2\mu \frac{\partial^2 r_1}{\partial T_0 \partial T_1} \theta_1 \\ &- J \frac{\partial^2 \theta_1}{\partial T_0^2} r_1 - 2J \frac{\partial^2 \theta_1}{\partial T_0 \partial T_1} - c_2 \frac{\partial x_1}{\partial T_0} - J \frac{\partial^2 \theta_2}{\partial T_0^2} - 4\mu \frac{\partial r_1}{\partial T_0} \frac{\partial \theta_1}{\partial T_1} + f_2 \cos(W_2 T_0), \end{aligned} \tag{17}$$

$$\begin{aligned} \frac{\partial^2 \theta_3}{\partial T_0^2} + \theta_3 &= -\frac{\partial^2 \theta_1}{\partial T_1^2} - 2 \frac{\partial^2 \theta_1}{\partial T_0 \partial T_1} - 2 \frac{\partial^2 \theta_2}{\partial T_0 \partial T_1} \\ &- r_1 \theta_2 - r_2 \theta_1 + 2r_1 \frac{\partial^2 \theta_1}{\partial T_0 \partial T_1} + r_2 \frac{\partial^2 \theta_1}{\partial T_0^2} \\ &- 2I \frac{\partial^2 x_1}{\partial T_0 \partial T_1} - 4 \frac{\partial^2 r_1}{\partial T_0^2} \frac{\partial^2 \theta_1}{\partial T_0 \partial T_1} - 4 \frac{\partial^2 r_1}{\partial T_0 \partial T_1} \frac{\partial^2 \theta_1}{\partial T_0^2} \\ &- 2r_1 \frac{\partial^2 r_1}{\partial T_0^2} \frac{\partial^2 \theta_1}{\partial T_0^2} - 2 \frac{\partial^2 x_1}{\partial T_0 \partial T_1} \\ &- r_2 \frac{\partial^2 \theta_1}{\partial T_0^2} - c_3 \frac{\partial \theta_1}{\partial T_0} + f_3 \cos(W_3 T_0). \end{aligned} \tag{18}$$

Equations (10–12) are mutually independent homogeneous equations. Thus, the polar forms of their solutions are as follows:

$$r_1 = A_1(T_1, T_2) e^{i\Omega_1 T_0} + \bar{A}_1(T_1, T_2) e^{-i\Omega_1 T_0}, \tag{19}$$

$$x_1 = A_2(T_1, T_2) e^{i\Omega_2 T_0} + \bar{A}_2(T_1, T_2) e^{-i\Omega_2 T_0}, \tag{20}$$

$$\theta_1 = A_3(T_1, T_2) e^{iT_0} + \bar{A}_3(T_1, T_2) e^{-iT_0}, \tag{21}$$

where  $A_1, A_2$ , and  $A_3$  are complex functions that can be determined later and  $\bar{A}_1, \bar{A}_2$ , and  $\bar{A}_3$  are their complex conjugate.

It is obvious that the solutions of (13–18) depend on the solutions of (10–12) significantly. Therefore, substituting the solutions (19–21) into (13–15) and removing terms that lead to the secular ones, we can get the second approximation in the form

$$r_2 = \frac{1}{\Omega_1^2} A_3 \bar{A}_3 - \frac{3A_3^2}{2\Omega_1^2 - 8} e^{2iT_0} + \Omega_2^2 A_3 \left( \frac{A_2 e^{i(1+\Omega_2)T_0}}{\Omega_1^2 - (1 + \Omega_2)^2} + \frac{\bar{A}_2 e^{i(1-\Omega_2)T_0}}{\Omega_1^2 - (1 - \Omega_2)^2} \right) + c.c., \tag{22}$$

$$x_2 = \mu A_1 (\Omega_1 + 2) \left( \frac{A_3 e^{i(\Omega_1+1)T_0}}{\Omega_2^2 - (\Omega_1 + 1)^2} + \frac{\bar{A}_3 e^{i(\Omega_2-1)T_0}}{\Omega_2^2 - (\Omega_1 - 1)^2} \right) + J \frac{A_3}{\Omega_2^2 - 1} e^{iT_0} + c.c., \tag{23}$$

$$\theta_2 = (3 - 2\Omega_1^2) A_1 \left( \frac{A_3 e^{i(\Omega_1+1)T_0}}{\Omega_1^2 + 2\Omega_1} + \frac{\bar{A}_3 e^{i(\Omega_1-1)T_0}}{\Omega_1^2 - 2\Omega_1} \right) + \frac{\Omega_2^2 A_3 I}{1 - \Omega_2^2} e^{i\Omega_2 T_0} + c.c., \tag{24}$$

where *c.c.* are the complex conjugate of the previous terms. This symbol benefits from providing long terms that we use frequently.

Substituting the solutions (19–24) into Eqs. (16–18) and using the elimination conditions of secular terms. So, one gets the third-order approximations in the forms

$$\begin{aligned} r_3 = & \frac{(3 - 2\Omega_1^2) A_1 A_3^2}{(\Omega_1^2 + 2\Omega_1)(4 + 4\Omega_1)} e^{i(\Omega_1+2)T_0} - \frac{6iA_3^2}{(\Omega_1^2 - 4)^2} e^{2iT_0} + \frac{\Omega_2^2 A_2 A_3 I e^{i(1+\Omega_2)T_0}}{(\Omega_2^2 - 1)[\Omega_1^2 - (1 + \Omega_2)^2]} \\ & - \left( \frac{(3 - 2\Omega_1^2)}{(\Omega_1^2 - 2\Omega_1)} + 1 \right) \frac{A_1 \bar{A}_3^2}{(4\Omega_1 - 4)} e^{i(\Omega_1-2)T_0} - \frac{\Omega_2^2 A_2 \bar{A}_3 I e^{i(\Omega_2-1)T_0}}{(1 - \Omega_2^2)[\Omega_1^2 - (\Omega_2 - 1)^2]} \\ & + \frac{A_1 A_3^2}{4\Omega_1 + 4} e^{i(\Omega_1+2)T_0} + \frac{\Omega_2^4 A_2^2 e^{2i\Omega_2 T_0}}{(1 - \Omega_2^2)(\Omega_1 - 4\Omega_2)} + \frac{(3 - 2\Omega_1^2) \Omega_2^2 A_1 A_2 A_3 e^{i(\Omega_1+\Omega_2+1)T_0}}{(\Omega_1^2 + 2\Omega_1)[\Omega_1^2 - (\Omega_1 + \Omega_2 + 1)^2]} \\ & + \frac{\Omega_2^4 A_2 \bar{A}_2 I}{(1 - \Omega_2^2) \Omega_1^2} + \frac{JA_3^2 e^{2iT_0}}{(1 - \Omega_2^2)(\Omega_1 - 4)} + \frac{\mu(\Omega_1 + 2)(\Omega_1 + 1)^2 A_1 A_3^2}{[\Omega_2^2 - (\Omega_1 + 1)^2](2\Omega_1 + 2)} e^{i(\Omega_1+2)T_0} \\ & + \frac{(3 - 2\Omega_1^2) \Omega_2^2 A_1 A_2 \bar{A}_3 e^{i(\Omega_1+\Omega_2-1)T_0}}{(\Omega_1^2 - 2\Omega_1)[\Omega_1^2 - (\Omega_1 + \Omega_2 - 1)^2]} + \frac{JA_3 \bar{A}_3}{(1 - \Omega_2^2) \Omega_1^2} + \frac{(3 - 2\Omega_1^2) \Omega_2^2 A_1 \bar{A}_2 A_3 e^{i(\Omega_1-\Omega_2+1)T_0}}{(\Omega_1^2 + 2\Omega_1)[\Omega_1^2 - (\Omega_1 - \Omega_2 + 1)^2]} \\ & + \frac{(3 - 2\Omega_1^2) \Omega_2^2 A_1 \bar{A}_2 \bar{A}_3 e^{i(\Omega_1-\Omega_2-1)T_0}}{(\Omega_1^2 - 2\Omega_1)[\Omega_1^2 - (\Omega_1 - \Omega_2 - 1)^2]} + \frac{f_1}{\Omega_1^2 - W_1^2} e^{iW_1 T_0} + c.c., \end{aligned} \tag{25}$$

$$\begin{aligned} x_3 = & \frac{\mu A_3^2 \bar{A}_3 e^{iT_0}}{(\Omega_2^2 - 1)} - \frac{\mu A_3^3 e^{3iT_0}}{(\Omega_2^2 - 9)} + \frac{(3 - 2\Omega_1^2) \mu \Omega_1 \bar{A}_1 A_3 i e^{i(1-2\Omega_1)T_0}}{(\Omega_1^2 + 2\Omega_1)[\Omega_2^2 - (1 - 2\Omega_1)^2]} + \frac{A_1 A_3 J e^{i(\Omega_1+1)T_0}}{[\Omega_2^2 - (\Omega_1 + 1)^2]} \\ & - \frac{(3 - 2\Omega_1^2) \mu \Omega_1 A_1^2 A_3 i e^{i(1+2\Omega_1)T_0}}{(\Omega_1^2 + 2\Omega_1)[\Omega_2^2 - (1 + 2\Omega_1)^2]} + \frac{\mu \Omega_1 \Omega_2^2 \bar{I} A_1 A_2 i e^{i(\Omega_2-\Omega_1)T_0}}{(1 - \Omega_2^2)[\Omega_2^2 - (\Omega_2 - \Omega_1)^2]} + \frac{A_1 \bar{A}_3 J e^{i(\Omega_1-1)T_0}}{[\Omega_2^2 - (\Omega_1 - 1)^2]} \\ & - \frac{\mu \Omega_1 \Omega_2^2 A_1 A_2 i e^{i(\Omega_1+\Omega_2)T_0}}{(1 - \Omega_2^2)[\Omega_2^2 - (\Omega_1 + \Omega_2)^2]} - (3 - 2\Omega_1^2) J \left\{ \frac{(\Omega_1 + 1) A_1 A_3 i e^{i(\Omega_1+1)T_0}}{(\Omega_1^2 + 2\Omega_1)[\Omega_2^2 - (\Omega_1 + 1)^2]} \right. \\ & \left. + \frac{(\Omega_1 - 1) A_1 \bar{A}_3 i e^{i(\Omega_1-1)T_0}}{(\Omega_1^2 - 2\Omega_1)[\Omega_2^2 - (\Omega_1 - 1)^2]} \right\} + \frac{f_2}{\Omega_2^2 - W_2^2} e^{iW_2 T_0} + c.c., \end{aligned} \tag{26}$$

$$\begin{aligned} \theta_3 = & \frac{(3 - 2\Omega_1^2)A_1^2A_3 i e^{i(1+2\Omega_1)T_0}}{(\Omega_1^2 + 2\Omega_1)(4\Omega_1^2 + 4\Omega_1)} - \frac{\Omega_2^2 A_1 A_2 I e^{i(\Omega_1 + \Omega_2)T_0}}{(1 - \Omega_2^2)[1 - (\Omega_1 + \Omega_2)^2]} - \frac{3A_3^3 e^{3iT_0}}{8(\Omega_1^2 - 4)} \\ & - \frac{\Omega_2^2 \bar{A}_1 A_2 I e^{i(\Omega_2 - \Omega_1)T_0}}{(1 - \Omega_2^2)[1 - (\Omega_2 - \Omega_1)^2]} - \frac{(3 - 2\Omega_1^2)A_1^2 \bar{A}_3 i e^{i(1+2\Omega_1)T_0}}{(\Omega_1^2 - 2\Omega_1)(4\Omega_1 - 4\Omega_1^2)} \\ & - 2 \frac{\Omega_2^2 A_3^2 A_2 e^{i(2+\Omega_2)T_0}}{[\Omega_1^2 - (1 + \Omega_2)^2](1 - (2 + \Omega_2)^2)} - 2 \frac{\Omega_2^2 A_3 \bar{A}_3 \bar{A}_2 e^{-i(\Omega_2)T_0}}{[\Omega_1^2 - (1 - \Omega_2)^2](1 + \Omega_2^2)} \\ & - 2 \frac{\Omega_1^2 A_1^2 \bar{A}_3 e^{i(2\Omega_1 - 1)T_0}}{1 - (2\Omega_1 - 1)^2} - \frac{3\Omega_2^2 A_3^2 A_2 e^{i(2+\Omega_2)T_0}}{2(\Omega_1^2 - 4)[1 - (2 + \Omega_2)^2]} - \frac{3\Omega_2^2 A_3^2 \bar{A}_2 e^{i(2-\Omega_2)T_0}}{2(\Omega_1^2 - 4)[1 - (2 - \Omega_2)^2]} \\ & + \frac{\Omega_2^2 A_3 \bar{A}_3 A_2 e^{-i\Omega_2 T_0}}{2(\Omega_1^2 - 4)[1 - (2 + \Omega_2)^2]} + \frac{\Omega_2^2 A_3 \bar{A}_3 \bar{A}_2 e^{-i\Omega_2 T_0}}{[\Omega_1^2 - (1 - \Omega_2)^2](1 + \Omega_2^2)} - \frac{3A_3^3 e^{3iT_0}}{2(\Omega_1^2 - 4)} \\ & + \frac{\Omega_2^2 \bar{A}_2^2 A_3 e^{i(1-2\Omega_2)T_0}}{[\Omega_1^2 - (1 - \Omega_2)^2][1 - (1 - 2\Omega_1)^2]} + \frac{\Omega_2^2 A_3^2 A_2 e^{i(2+\Omega_2)T_0}}{[\Omega_1^2 - (1 + \Omega_2)^2][1 - (1 + \Omega_2)^2]} \\ & + \frac{\Omega_2^2 A_3^2 \bar{A}_2 e^{i(2-\Omega_2)T_0}}{[\Omega_1^2 - (1 - \Omega_2)^2][1 - (2 - \Omega_2)^2]} + \frac{\Omega_2^2 A_2^2 A_3 e^{i(1+2\Omega_2)T_0}}{[\Omega_1^2 - (1 + \Omega_2)^2][1 - (1 + 2\Omega_2)^2]} \\ & + \frac{f_3}{1 - W_3^2} e^{iW_3 T_0} + c.c. \end{aligned} \tag{27}$$

Thus, the required approximate solutions can be easily obtained if we substitute (19–27) into (8).

### Stability of the System

In this section, we examine the system’s stability of Eqs. (16–18) and investigate the simultaneous three primary external resonances case. Therefore, the following detuning parameters  $\sigma_j$  ( $j = 1, 2, 3$ ) are considered [30]

$$W_1 = \Omega_1 + \varepsilon\sigma_1, \quad W_2 = \Omega_2 + \varepsilon\sigma_2, \quad W_3 = 1 + \varepsilon\sigma_3. \tag{28}$$

Substituting (28) into (13–18) and removing the secular terms, the following solvability requirements for the third-order approximation are obtained

$$\begin{aligned} -2i\Omega_1 \frac{\partial A_1}{\partial T_2} - \frac{(3 - 2\Omega_1^2)}{(\Omega_1^2 - 2\Omega_1)} A_1 A_3 \bar{A}_3 - \frac{(3 - 2\Omega_1^2)}{(\Omega_1^2 + 2\Omega_1)} A_1 A_3 \bar{A}_3 + 2A_1 A_3 \bar{A}_3 \\ - \frac{(\Omega_1 - 1)^2}{(\Omega_2^2 - (\Omega_1 - 1)^2)} A_1 A_3 \bar{A}_3 - i c_1 \Omega_1 A_1 - \frac{1}{2} f_1 e^{i\sigma_1 T_1} = 0, \end{aligned} \tag{29}$$

$$-2i\Omega_2 \frac{\partial A_2}{\partial T_2} - \frac{\Omega_2^4 J I A_2}{(1 - \Omega_2^2)} - i c_2 \Omega_2 A_2 - \frac{1}{2} f_2 e^{i\sigma_2 T_1} = 0, \tag{30}$$

$$\begin{aligned} -2i \frac{\partial A_3}{\partial T_2} - \frac{(3 - 2\Omega_1^2)}{(\Omega_1^2 + 2\Omega_1)} A_1 A_3 \bar{A}_1 - i c_3 A_3 \\ - 4\Omega_1^2 A_1 A_3 \bar{A}_1 + \frac{\Omega_2^4 A_2 A_3 \bar{A}_2}{\Omega_1^2 - (\Omega_2 + 1)^2} \\ + \frac{\Omega_2^4 A_2 A_3 \bar{A}_2}{\Omega_1^2 - (1 - \Omega_2)^2} - \frac{1}{2} f_3 e^{i\sigma_3 T_1} = 0. \end{aligned} \tag{31}$$

These equations can be analyzed through expressing  $A_j$  ( $j = 1, 2, 3$ ) in the polar forms [31] as follows:

$$A_i = \frac{\tilde{a}_j(T_2)}{2} e^{i\tilde{\psi}_j T_2}, \quad a_j = \varepsilon \tilde{a}_j, \tag{32}$$

where  $\tilde{a}_j$  and  $\tilde{\psi}_j$  are the amplitudes of the generalized coordinates  $r$ ,  $x$ , and  $\theta$  and their corresponding phases

$$\frac{\partial A_j}{\partial T} = \varepsilon^2 \frac{\partial A_j}{\partial T_2}, \tag{33}$$

$$\theta_j(T_1, T_2) = T_j \tilde{\sigma}_j - \psi_j(T_2). \tag{34}$$

Substituting (32–34) into (29–31) and then matching the real and imaginary parts in both sides to gain the next modulation equations for amplitudes and phases

$$\begin{aligned}
 a_1 \frac{d\theta_1}{dT} &= \frac{a_1 a_3^2}{4\Omega_1} - \left( \frac{1}{\Omega_1^2 - 2\Omega_1} + \frac{1}{\Omega_1^2 + 2\Omega_1} \right) \frac{(3 - 2\Omega_1^2)a_1 a_3^2}{8\Omega_1} + a_1 \sigma_1 \\
 &\quad - \frac{(\Omega_1 - 1)^2 a_1 a_3^2}{8\Omega_1(\Omega_2^2 - (\Omega_1 - 1)^2)} + \frac{f_1}{2\Omega_1} \cos \theta_1, \\
 \frac{d a_1}{dT} &= \frac{f_1}{2\Omega_1} \sin \theta_1 - \frac{a_1 c_1}{2}, \\
 a_2 \frac{d\theta_2}{dT} &= \frac{f_2}{2\Omega_2} \cos \theta_2 - \frac{J I a_2 \Omega_2^3}{2(1 - \Omega_2^2)} + a_2 \sigma_2, \\
 \frac{d a_2}{dT} &= \frac{f_2}{2\Omega_2} \sin \theta_2 - \frac{a_2 c_2}{2}, \\
 a_3 \frac{d\theta_3}{dT} &= \frac{\Omega_2^4 a_3 a_2^2}{8(\Omega_1^2 - (1 + \Omega_2)^2)} - \frac{(3 - 2\Omega_1^2)a_3 a_1^2}{8(\Omega_1^2 + 2\Omega_1)} - \frac{1}{2} \Omega_1^2 a_3 a_1^2 \\
 &\quad + \frac{\Omega_2^4 a_3 a_2^2}{8(\Omega_1^2 - (1 - \Omega_2)^2)} + a_3 \sigma_3 + \frac{f_3}{2} \cos \theta_3, \\
 \frac{d a_3}{dT} &= \frac{f_3}{2} \sin \theta_3 - \frac{a_3 c_3}{2}.
 \end{aligned} \tag{35}$$

Examining the behavior of modest deviations from the steady-state solutions is an intriguing way to evaluate the stability requirements. Therefore, we take into account the following aspects of substitutions [32] when pursuing this goal

$$\begin{aligned}
 a_1 &= a_{10} + a_{11}, & \theta_1 &= \theta_{10} + \theta_{11}, \\
 a_2 &= a_{20} + a_{21}, & \theta_2 &= \theta_{20} + \theta_{21}, \\
 a_3 &= a_{30} + a_{31}, & \theta_3 &= \theta_{30} + \theta_{31},
 \end{aligned} \tag{36}$$

where  $a_{j0}$  and  $\theta_{j0}$  ( $j = 1, 2, 3$ ) are the unperturbed solutions which corresponds to the steady-state solutions of (35), while  $a_{j1}$  and  $\theta_{j1}$  are their corresponding perturbations which should be small relative to its predecessors.

Substitution (36) into Eq. (35) yields

$$\begin{aligned}
 a_{10} \frac{d\theta_{11}}{dT} &= \left( \frac{1}{4\Omega_1} - \frac{(\Omega_1 - 1)^2}{8\Omega_1(\Omega_2^2 - (\Omega_1 - 1)^2)} \right) \\
 &\quad - \left( \frac{1}{\Omega_1^2 - 2\Omega_1} + \frac{1}{\Omega_1^2 + 2\Omega_1} \right) \times \frac{(3 - 2\Omega_1^2)}{8\Omega_1} \\
 &\quad (a_{11} a_{30}^2 + 2a_{10} a_{31} a_{30}) \\
 &\quad - \frac{f_1}{2\Omega_1} \sin \theta_{10} \theta_{11} + a_{11} \sigma_1, \\
 \frac{d a_{11}}{dT} &= \frac{f_1}{2\Omega_1} \cos \theta_{10} \theta_{11} - \frac{a_{11} c_1}{2}, \\
 a_{20} \frac{d\theta_{21}}{dT} &= a_{21} \sigma_2 - \frac{f_2}{2\Omega_2} \sin \theta_{20} \theta_{21} - \frac{J I a_{21} \Omega_2^3}{2(1 - \Omega_2^2)}, \\
 \frac{d a_{21}}{dT} &= \frac{f_2}{2\Omega_2} \cos \theta_{20} \theta_{21} - \frac{a_{21} c_2}{2}, \\
 a_{30} \frac{d\theta_{30}}{dT} &= \frac{f_3}{2} \sin \theta_{30} \theta_{31} + a_{31} \sigma_3 \\
 &\quad - \left( \frac{(3 - 2\Omega_1^2)}{8(\Omega_1^2 + 2\Omega_1)} + \frac{1}{2} \Omega_1^2 (a_{31} a_{10}^2 + 2a_{10} a_{11} a_{30}) \right) \\
 &\quad + \frac{\Omega_2^4}{8} \left( \frac{1}{(\Omega_1^2 - (1 - \Omega_2)^2)} + \frac{1}{(\Omega_1^2 - (1 + \Omega_2)^2)} \right) \\
 &\quad (a_{31} a_{20}^2 + 2a_{20} a_{21} a_{30}), \\
 \frac{d a_{31}}{dT} &= \frac{f_3}{2} \cos \theta_{30} \theta_{31} - \frac{a_{31} c_3}{2}.
 \end{aligned} \tag{37}$$

It must be remembered that the perturbation terms  $a_{j1}$  and  $\theta_{j1}$  are unknown functions and we can express their solutions in the exponential form  $c_k e^{\lambda T}$ ; in which  $c_k$  ( $k = 1, 2, \dots, 6$ ) are constants and  $\lambda$  represents the eigenvalue congruent to the unknown perturbations that can be obtained from the real parts of the roots. If the steady-state solutions  $a_{j0}$  and  $\theta_{j0}$  are considered to be stable asymptotically, then the real components of the roots of the below characteristic equation must be negative [33]

$$\lambda^6 + \Gamma_1 \lambda^5 + \Gamma_2 \lambda^4 + \Gamma_3 \lambda^3 + \Gamma_4 \lambda^2 + \Gamma_5 \lambda + \Gamma_6 = 0, \tag{38}$$

where

The previous coefficients  $\Gamma_k$  ( $k = 1, 2, \dots, 6$ ) depend on some parameters such as  $a_{j0}$ ,  $\theta_{j0}$ ,  $c_k$  and  $f_j$  ( $j = 1, 2, 3$ ). Based on the Routh-Hurwitz criterion [16, 34],

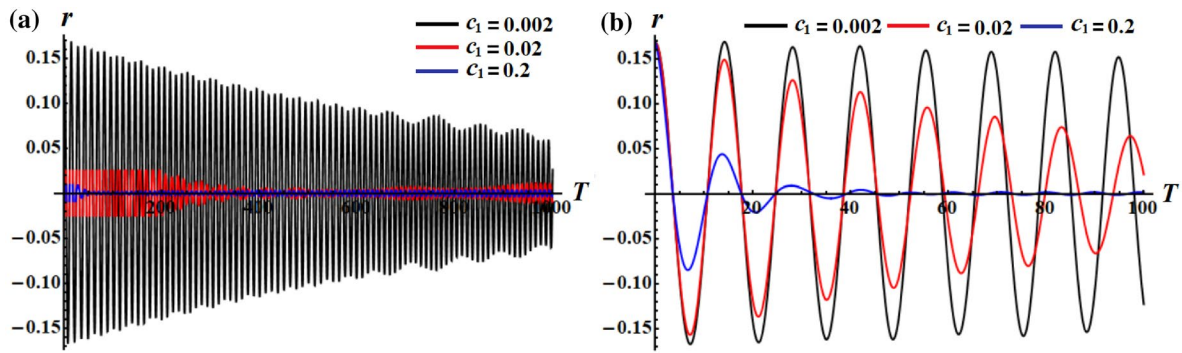


Fig. 2 The slight effect of  $c_1$  on the behavior of the solution  $r$  when  $c_1 = (0.002, 0.02, 0.2)$ : **a** at  $T \in [0, 1000]$ , **b** at  $T \in [0, 100]$

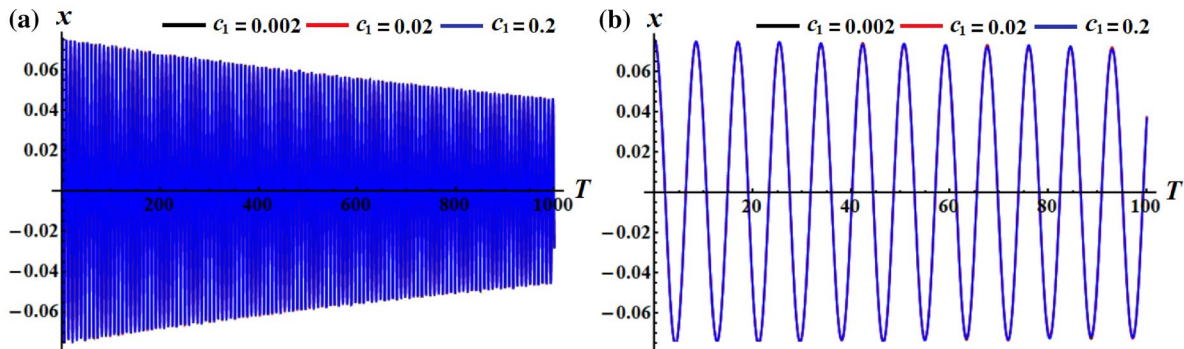


Fig. 3 The slight effect of  $c_1$  on the behavior of the solution  $x$  when  $c_1 = (0.002, 0.02, 0.2)$ : **a** at  $T \in [0, 1000]$ , **b** at  $T \in [0, 100]$

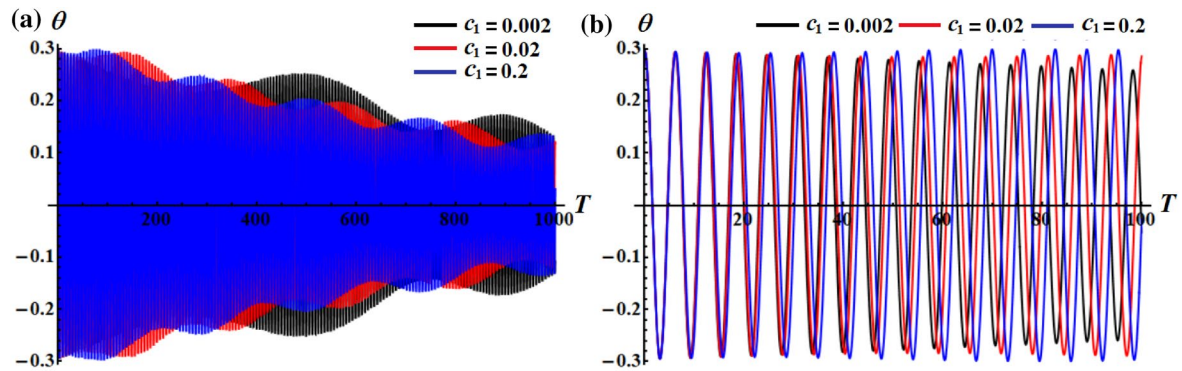


Fig. 4 The effect of  $c_1$  on the behavior of the solution  $\theta$  when  $c_1 = (0.002, 0.02, 0.2)$ : **a** at  $T \in [0, 1000]$ , **b** at  $T \in [0, 100]$

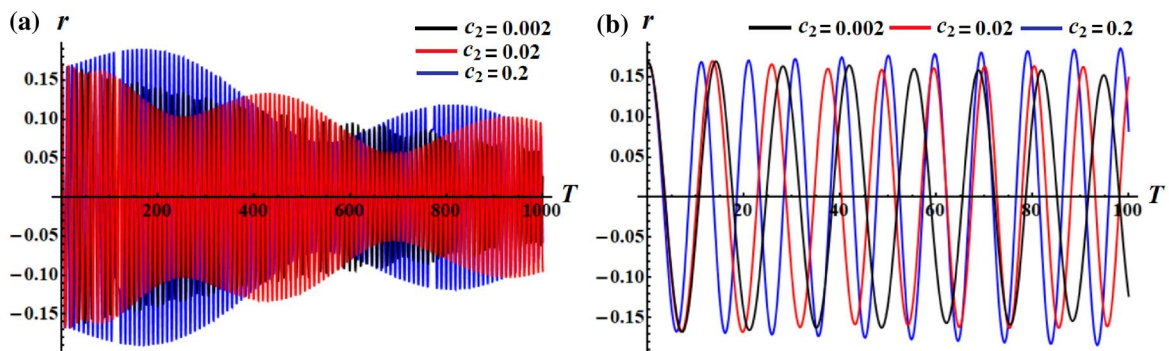
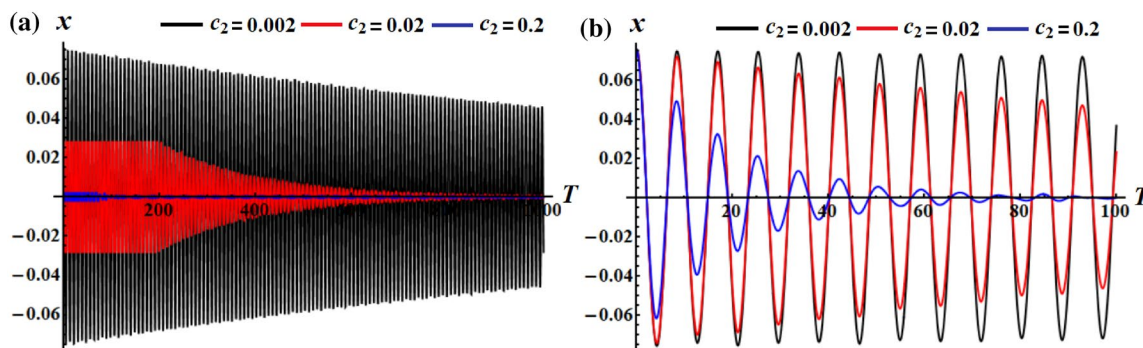
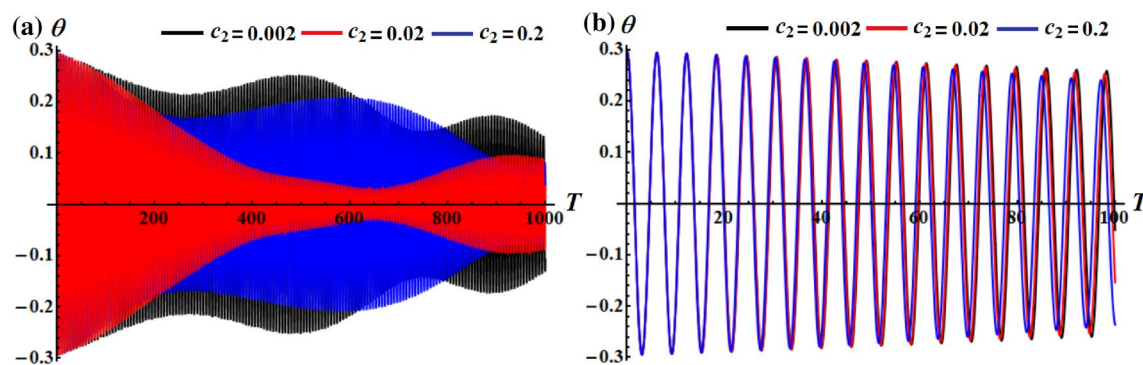


Fig. 5 The effect  $c_2$  on the behavior of the solution  $r$  when  $c_2 = (0.002, 0.02, 0.2)$ : **a** at  $T \in [0, 1000]$ , **b** at  $T \in [0, 100]$





**Fig. 6** The slight effect of  $c_2$  on the behavior of the solution  $x$  when  $c_2 = (0.002, 0.02, 0.2)$ : **a** at  $T \in [0, 1000]$ , **b** at  $T \in [0, 100]$



**Fig. 7** The slight effect of  $c_2$  on the behavior of the solution  $\theta$  when  $c_2 = (0.002, 0.02, 0.2)$ : **a** at  $T \in [0, 1000]$ , **b** at  $T \in [0, 100]$

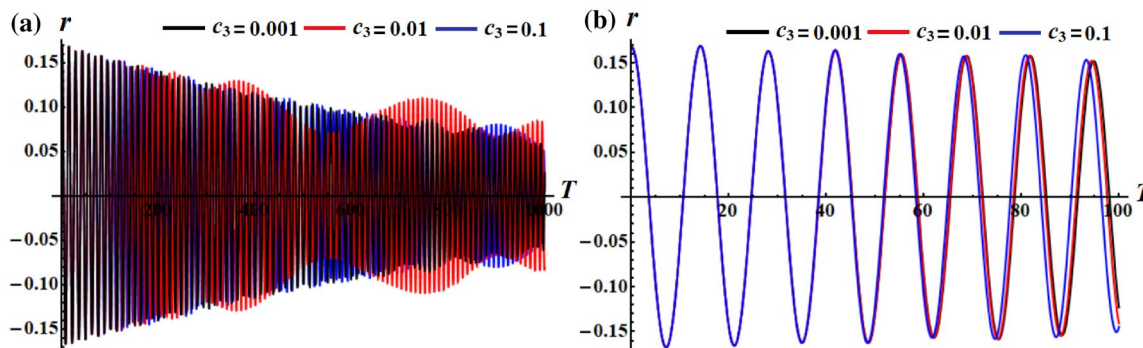


**Fig. 8** The slight effect of  $c_3$  on the behavior of the solution  $r$  when  $c_3 = (0.001, 0.01, 0.1)$ : **a** at  $T \in [0, 1000]$ , **b** at  $T \in [0, 100]$

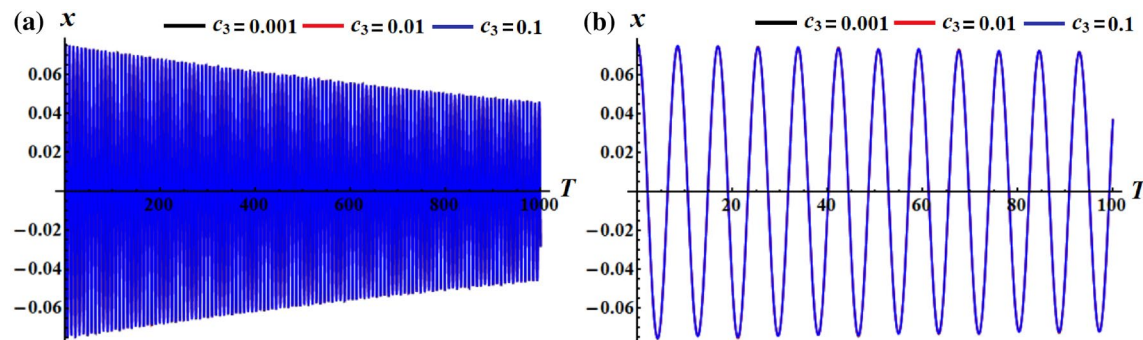


**Fig. 9** The effect of  $c_3$  on the behavior of the solution  $x$  when  $c_3 = (0.001, 0.01, 0.1)$ : **a** at  $T \in [0, 1000]$ , **b** at  $T \in [0, 100]$

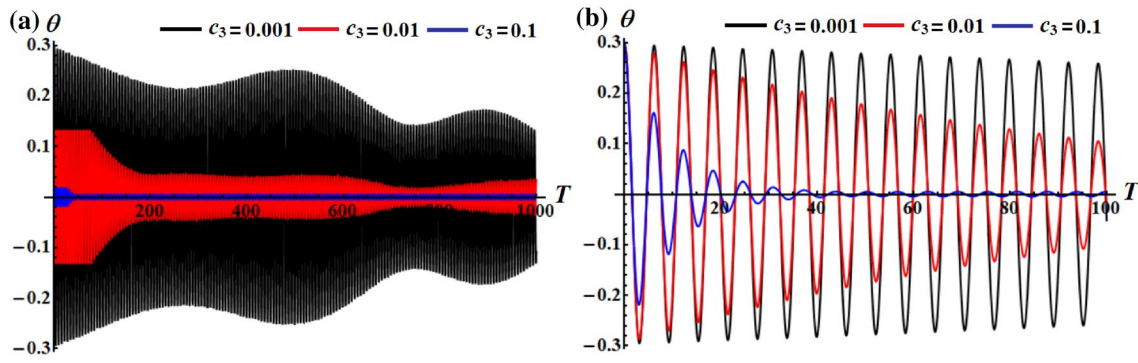


**Fig. 10** The slight effect of  $c_3$  on the behavior of the solution  $\theta$  when  $c_3 = (0.001, 0.01, 0.1)$ : **a** at  $T \in [0, 1000]$ , **b** at  $T \in [0, 100]$

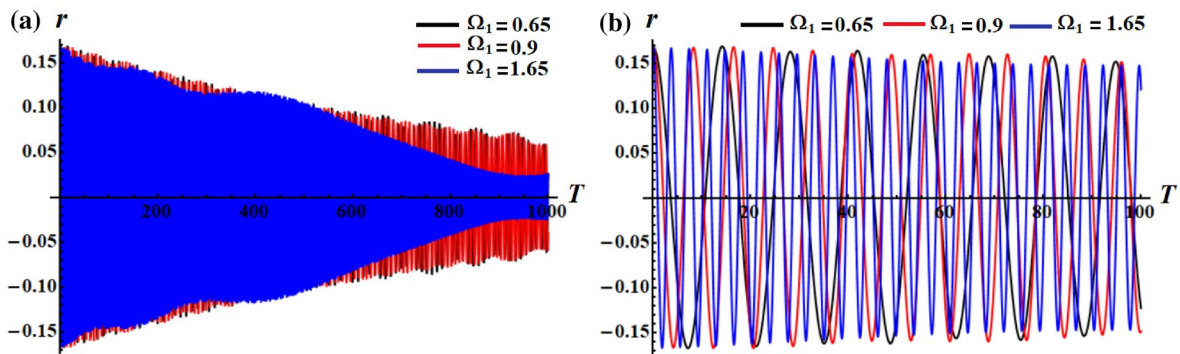


**Fig. 11** The effect of  $\Omega_1$  on the behavior of the solution  $r$  when  $\Omega_1 = (0.65, 0.9, 1.65)$ : **a** at  $T \in [0, 1000]$ , **b** at  $T \in [0, 100]$

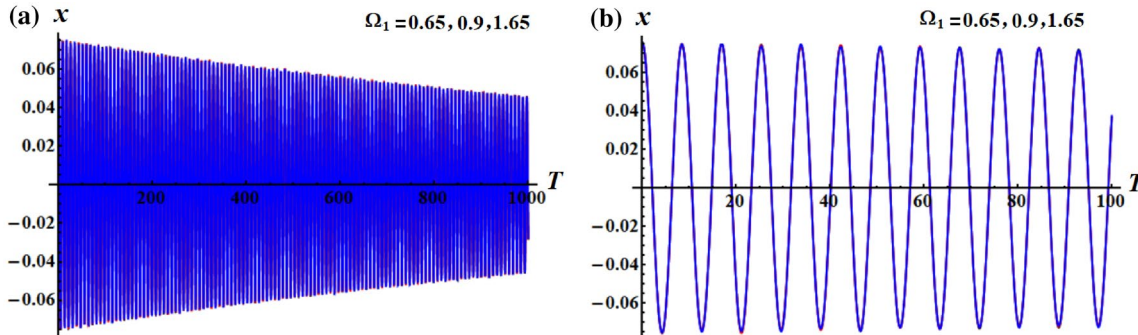


**Fig. 12** The slight effect of  $\Omega_1$  on the behavior of the solution  $x$  when  $\Omega_1 = (0.65, 0.9, 1.65)$ : **a** at  $T \in [0, 1000]$ , **b** at  $T \in [0, 100]$

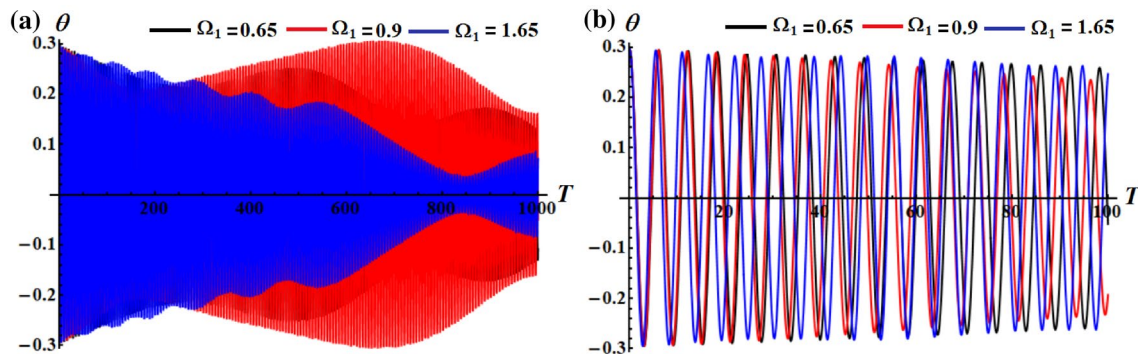


**Fig. 13** The slight effect of  $\Omega_1$  on the behavior of the solution  $\theta$  when  $\Omega_1 = (0.65, 0.9, 1.65)$ : **a** at  $T \in [0, 1000]$ , **b** at  $T \in [0, 100]$

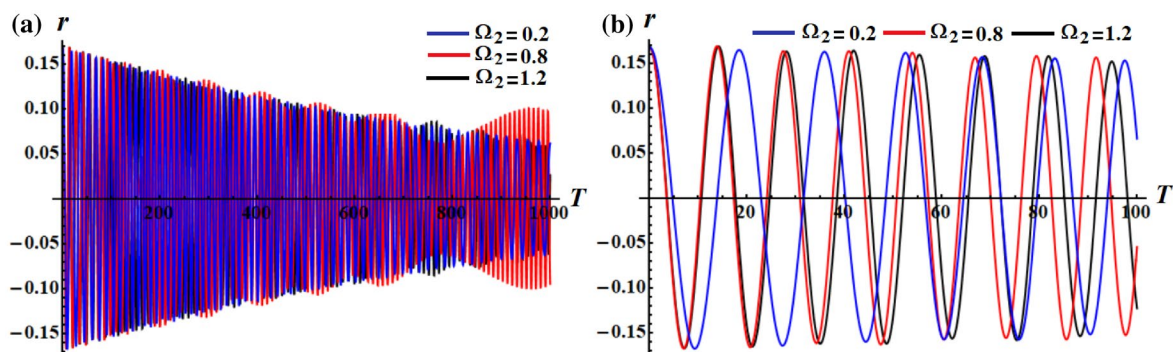


Fig. 14 The slight effect of  $\Omega_2$  on the behavior of the solution  $r$  when  $\Omega_2 = (0.2, 0.8, 1.2)$ : **a** at  $T \in [0, 1000]$ , **b** at  $T \in [0, 100]$

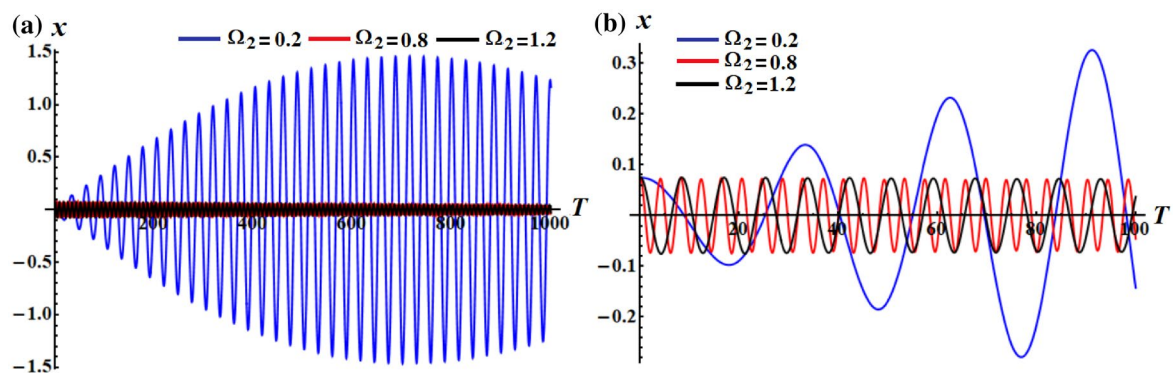


Fig. 15 The slight effect of  $\Omega_2$  on the behavior of the solution  $x$  when  $\Omega_2 = (0.2, 0.8, 1.2)$ : **a** at  $T \in [0, 1000]$ , **(b)** at  $T \in [0, 100]$

$$Det_k \begin{pmatrix} \Gamma_1 & 1 & 0 & 0 & \dots & 0 \\ \Gamma_3 & \Gamma_2 & \Gamma_1 & 1 & \dots & 0 \\ \Gamma_5 & \Gamma_4 & \Gamma_3 & \Gamma_2 & \dots & 0 \\ \Gamma_7 & \Gamma_6 & \Gamma_5 & \Gamma_4 & \dots & 0 \\ \vdots & \vdots & \vdots & \vdots & \vdots & \vdots \\ \Gamma_{2k-1} & \Gamma_{2k-2} & \Gamma_{2k-3} & \dots & \dots & \Gamma_k \end{pmatrix}$$

we can write the stability conditions of the steady-state solutions in the following form:

$$\begin{aligned} & \Gamma_1 > 0, & & Det \begin{pmatrix} \Gamma_1 & 1 \\ \Gamma_3 & \Gamma_2 \end{pmatrix} > 0 \\ & Det \begin{pmatrix} \Gamma_1 & 1 & 0 \\ \Gamma_3 & \Gamma_2 & \Gamma_1 \\ \Gamma_5 & \Gamma_4 & \Gamma_3 \end{pmatrix} > 0, & & Det \begin{pmatrix} \Gamma_1 & 1 & 0 & 0 \\ \Gamma_3 & \Gamma_2 & \Gamma_1 & 1 \\ \Gamma_5 & \Gamma_4 & \Gamma_3 & \Gamma_2 \\ 0 & \Gamma_6 & \Gamma_5 & \Gamma_4 \end{pmatrix} > 0, \\ & Det \begin{pmatrix} \Gamma_1 & 1 & 0 & 0 & 0 \\ \Gamma_3 & \Gamma_2 & \Gamma_1 & 1 & 0 \\ \Gamma_5 & \Gamma_4 & \Gamma_3 & \Gamma_2 & \Gamma_1 \\ 0 & \Gamma_6 & \Gamma_5 & \Gamma_4 & \Gamma_3 \\ 0 & 0 & 0 & \Gamma_6 & \Gamma_5 \end{pmatrix} > 0, & & Det \begin{pmatrix} \Gamma_1 & 1 & 0 & 0 & 0 & 0 \\ \Gamma_3 & \Gamma_2 & \Gamma_1 & 1 & 0 & 0 \\ \Gamma_5 & \Gamma_4 & \Gamma_3 & \Gamma_2 & \Gamma_1 & 1 \\ 0 & \Gamma_6 & \Gamma_5 & \Gamma_4 & \Gamma_3 & \Gamma_2 \\ 0 & 0 & 0 & \Gamma_6 & \Gamma_5 & \Gamma_4 \\ 0 & 0 & 0 & 0 & 0 & \Gamma_6 \end{pmatrix} > 0. \end{aligned} \tag{40}$$

### Simulation of the Results

Now, we are going to investigate the influence of the parameters  $c_1, c_2, c_3, \Omega_1$ , and  $\Omega_2$  on the motion of the system under investigation taking into the following value of different parameters:

$$\begin{aligned} & c_1 = (0.002, 0.02, 0.2), \quad f_1 = 0.003, \quad \sigma_1 = 0.01, \quad c_2 = 0.002, \\ & c_3 = 0.001, \quad \Omega_1 = 0.65, \quad \sigma_2 = 0.02, \quad m = 0.5 \text{ kg}, \quad M^* = 1 \text{ kg}, \\ & W_1 = 0.2, \quad W_2 = 0.1, \quad \Omega_2 = 1.2, \quad f_1 = 0.001, \quad f_1 = 0.002, \\ & W_3 = 0.3, \quad \epsilon = 0.001. \end{aligned}$$

Figures 2, 3, 4 represent the variation of the solutions  $r, x$ , and  $\theta$  via  $T$ , respectively, when  $c_1 = (0.002, 0.02, 0.2)$  with the same previous data, during the specified time  $T$  intervals for each figure. Whereas Figs. 5, 6, 7 indicate the behavior of the solutions  $r, x$ , and  $\theta$  at  $c_2 = (0.002, 0.02, 0.2)$ .

A look at Fig. 2 reveals that when  $c_1$  increases from 0.002 to 0.2 with the constancy of other parameters and the number of oscillations decreases with the notable increment of the amplitudes. This means that through variation of time  $T$  from 0 to 100, the motion of the mass  $m$  is sinusoidal. On the other hand, the amplitudes of  $x$  and  $\theta$  during the same time interval decrease. There is decay in the variation of

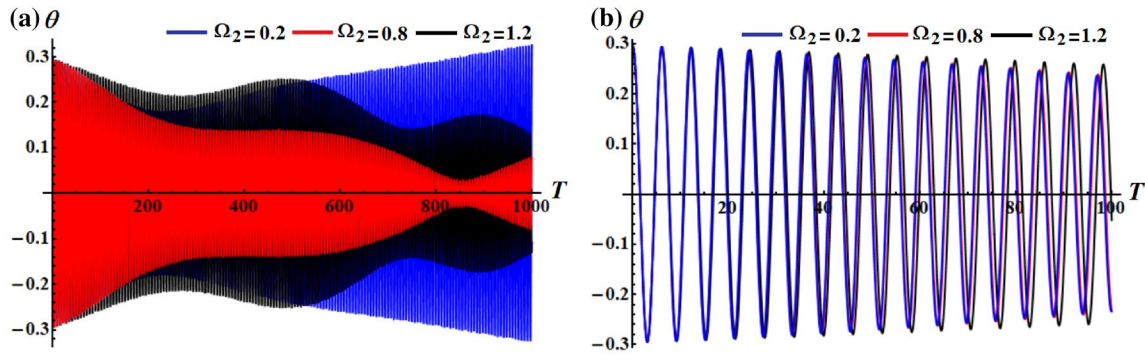


**Fig. 16** The slight effect of  $\Omega_2$  on the behavior of the solution  $\theta$  when  $\Omega_2 = (0.2, 0.8, 1.2)$ : **a** at  $T \in [0, 1000]$ , **b** at  $T \in [0, 100]$

**Fig. 17** Adjustment of the modified amplitudes as a function of the detuning parameter  $\sigma_3$

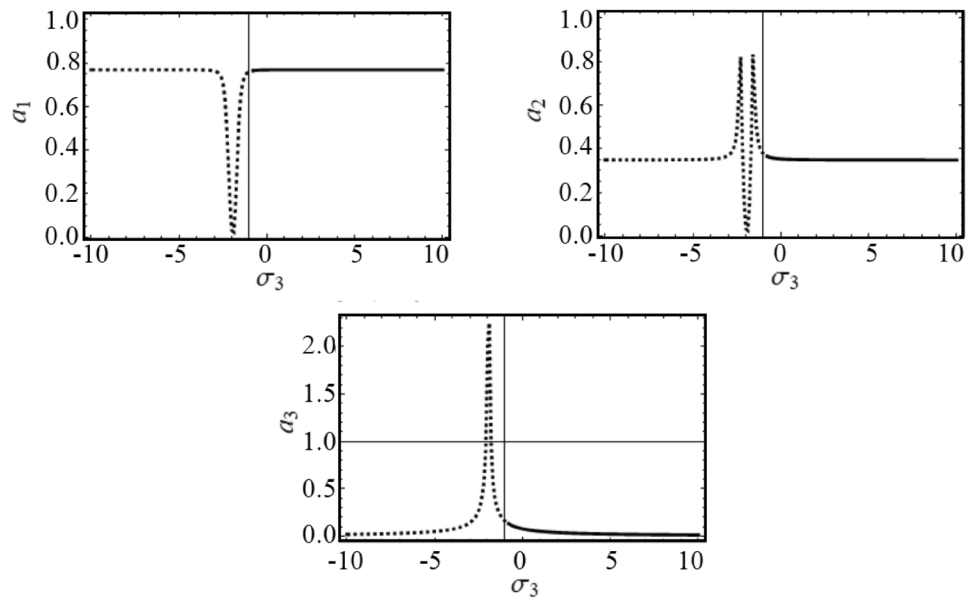


**Fig. 18** The modified amplitudes' variation for the same case in Fig. 17, but when  $c_2 = 0.02$ .

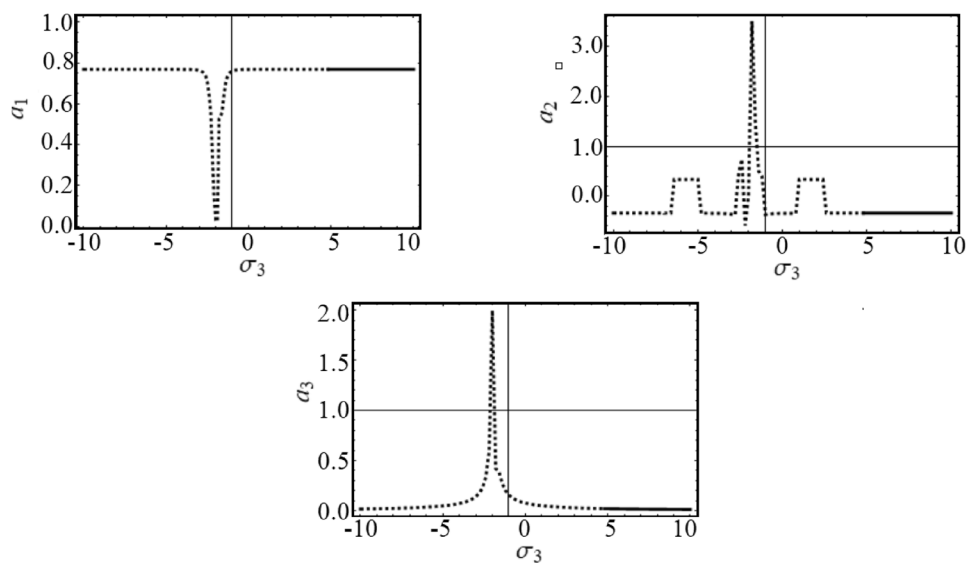


**Fig. 19** The modified amplitudes vs the parameter of detuning  $\sigma_3$  for the same case in Fig. 17, but when  $c_3 = 0.001$ .

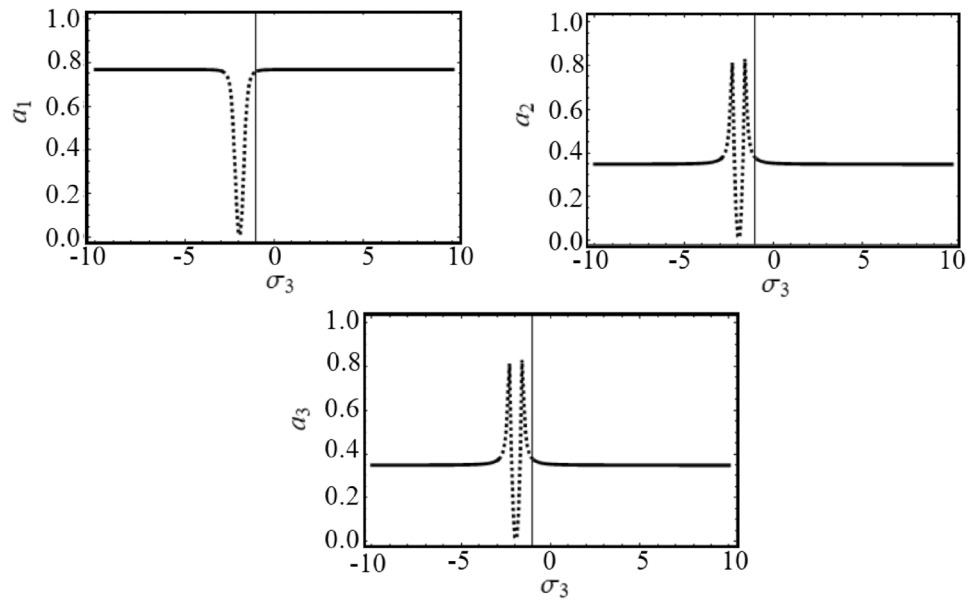


**Fig. 20** The modified amplitudes vs the parameter of detuning  $\sigma_3$  for the same case in Fig. 17, but when  $\sigma_1 = -1$ .

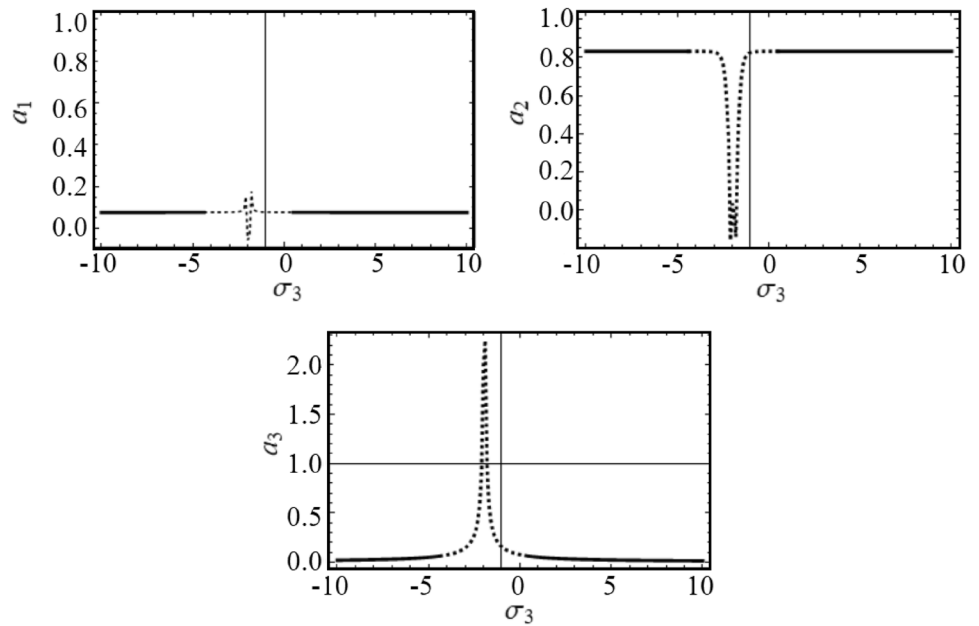


**Fig. 21** The modified amplitudes vs the parameter of detuning  $\sigma_3$  for the same case in Fig. 17, but when  $\sigma_2 = -0.005$ .

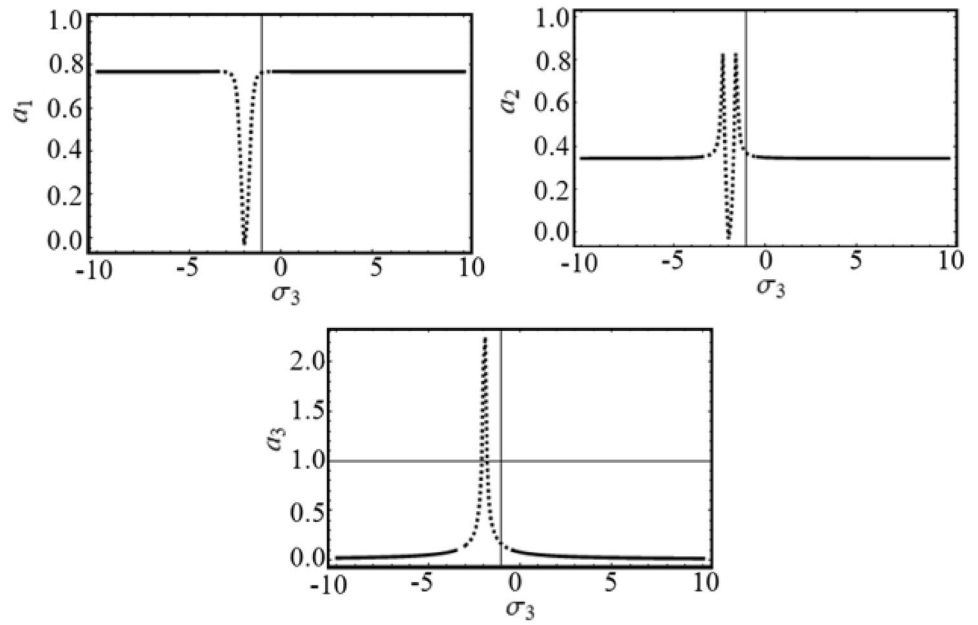


**Fig. 22** The trajectory of the modulation equation's projection on plane  $p_2q_2$  and the adjusted amplitudes via time  $T_2$

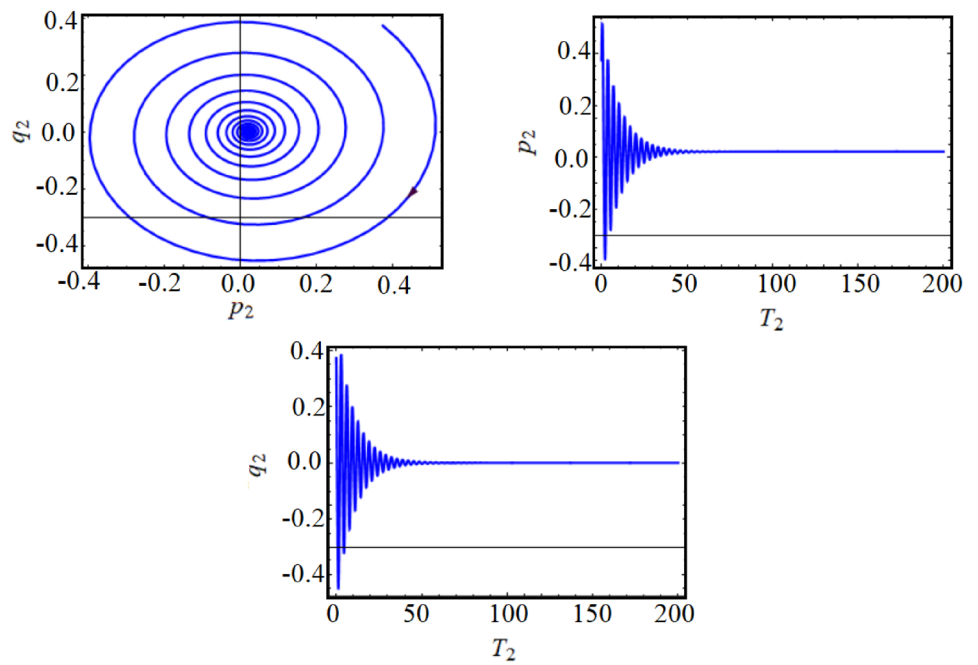


**Fig. 23** The same system considered in Fig. 22, but with  $c_2 = 0.02$

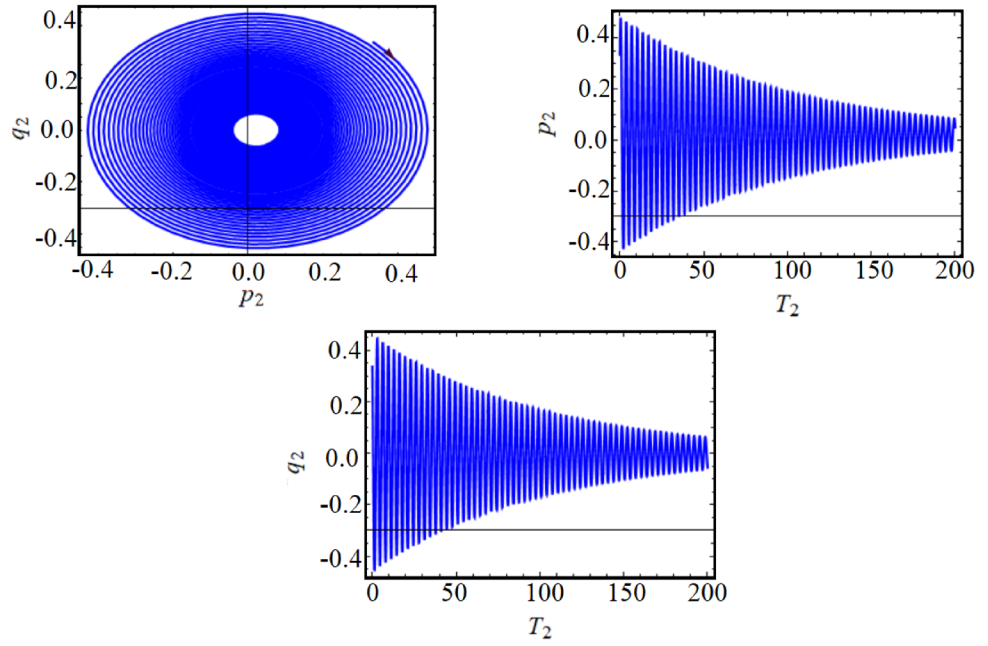


**Fig. 24** The projection  $p_2q_2$  plane and the corresponding modified amplitudes with  $c_3 = 0.001$ , and it is corresponding to the first fixed point in Fig. 19

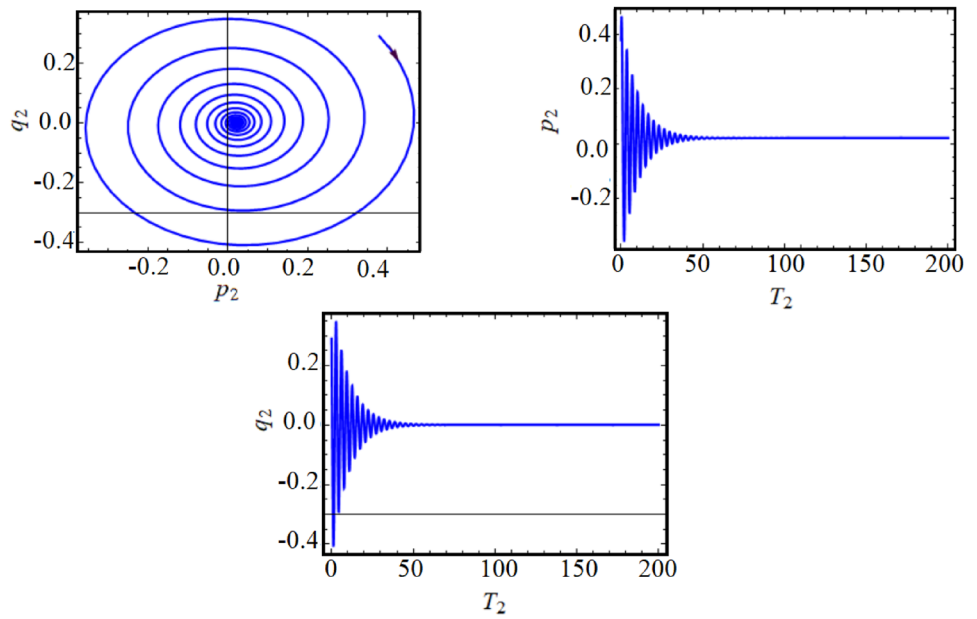


**Fig. 25** The projection  $p_2q_2$  plane and the corresponding modified amplitudes where  $c_3 = 0.001$  corresponding to the second fixed point in Fig. 19

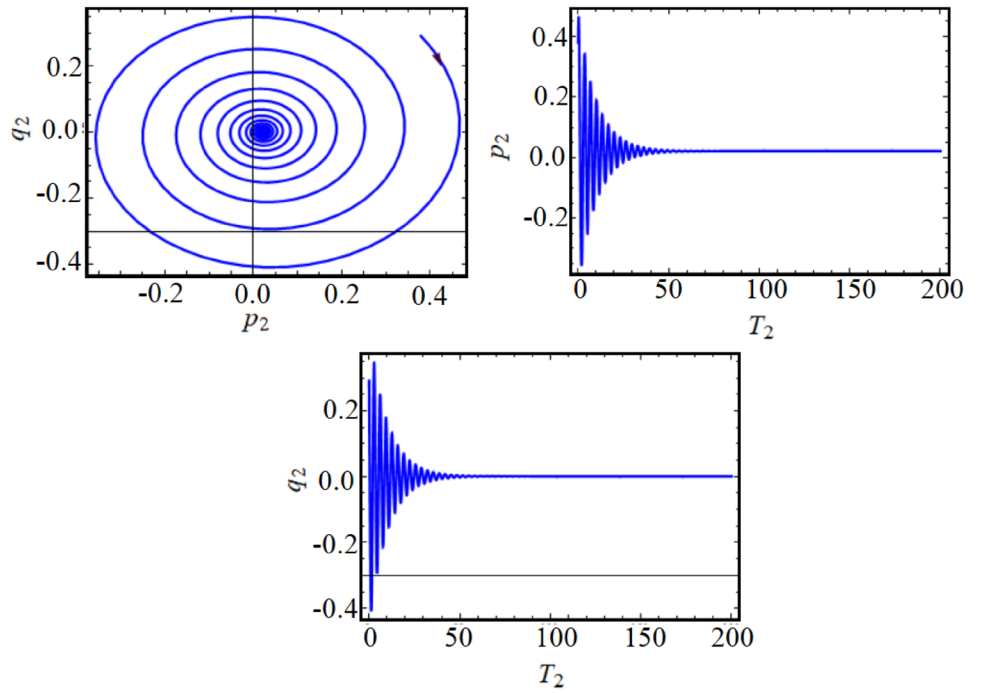


**Fig. 26** The projection of the modulation equation path on the plane  $p_2q_2$  and the adjusted amplitudes versus  $T_2$  at  $\sigma_1 = -1$ , and it is corresponding first point in Fig. 20

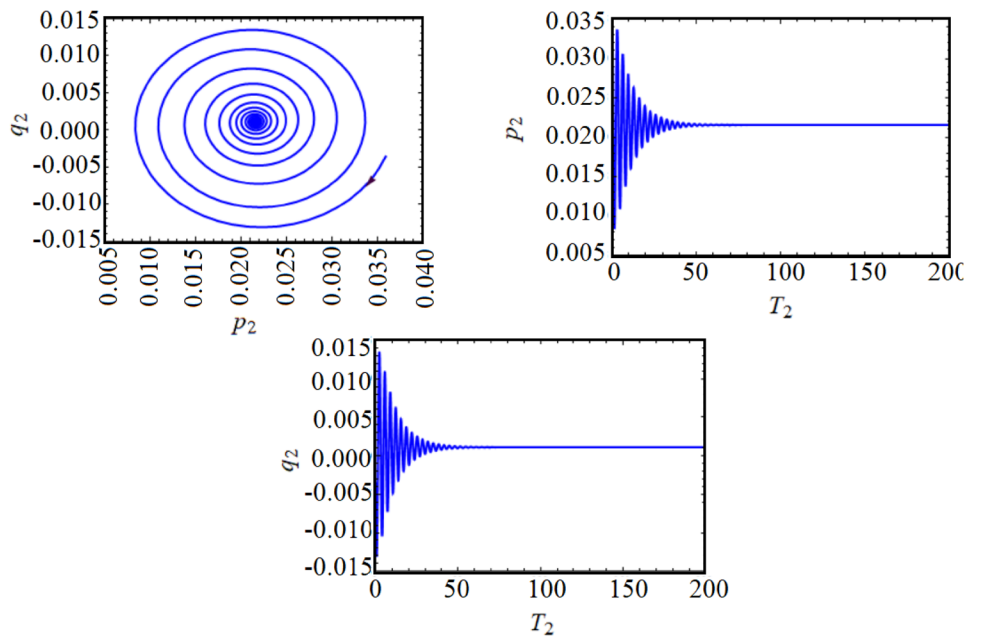




**Fig. 27** The projection of the equation of modulation on the phase plane  $p_2q_2$  and the adjusted amplitudes versus  $T_2$  at  $\sigma_1 = -1$ , and it is corresponding second fixed point in Fig. 20

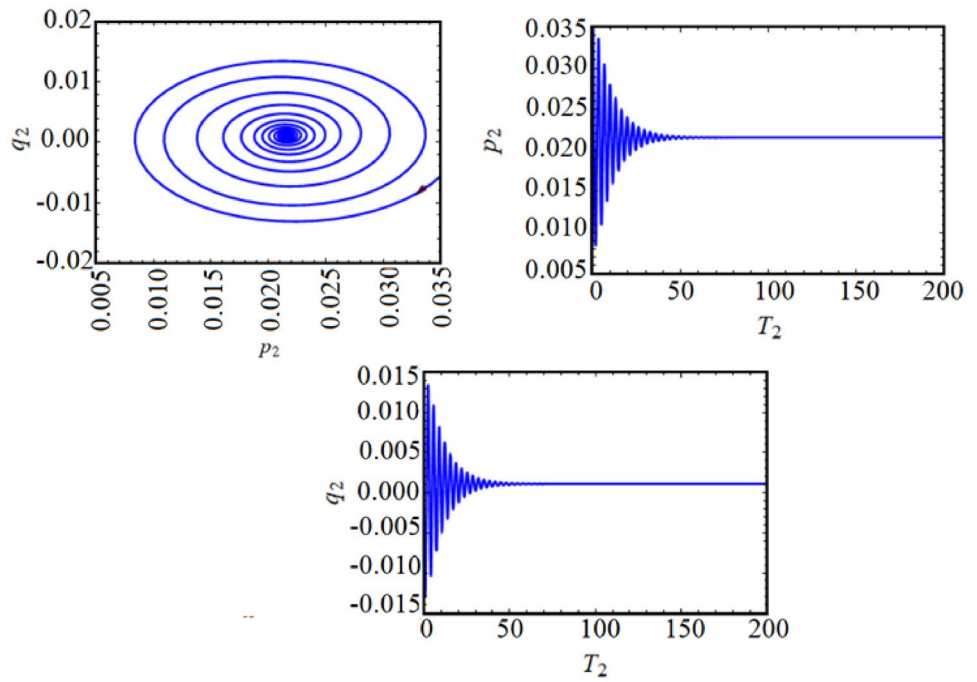


**Fig. 28** The projection of the modulation equation trajectory on the plane  $p_2q_2$  and the adjusted amplitudes versus  $T_2$  at  $\sigma_2 = -0.005$ , and it is corresponding first fixed point in Fig. 21

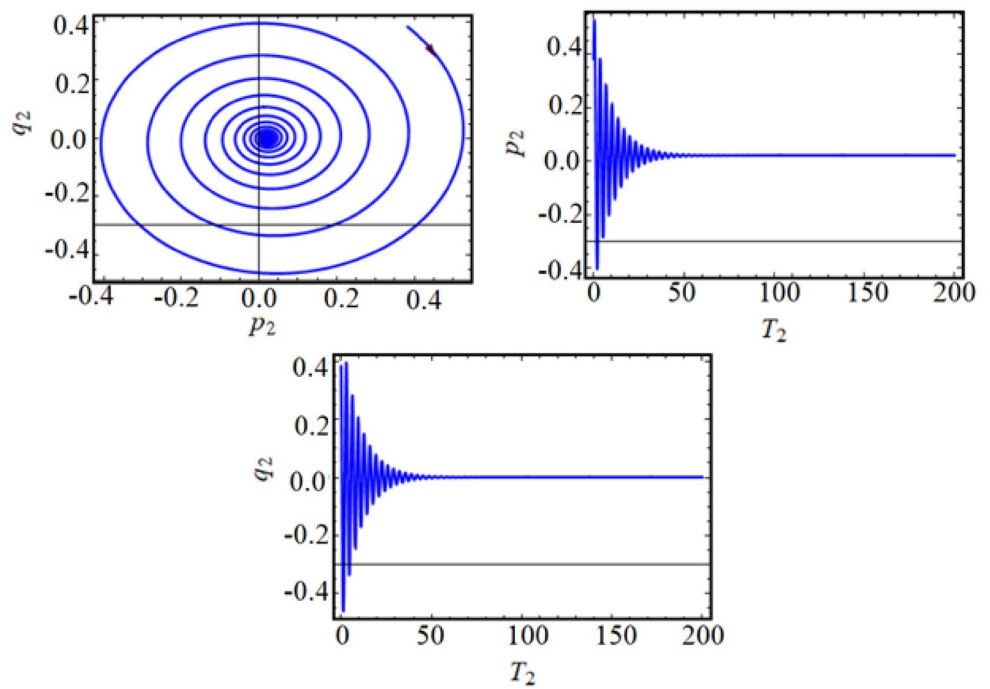
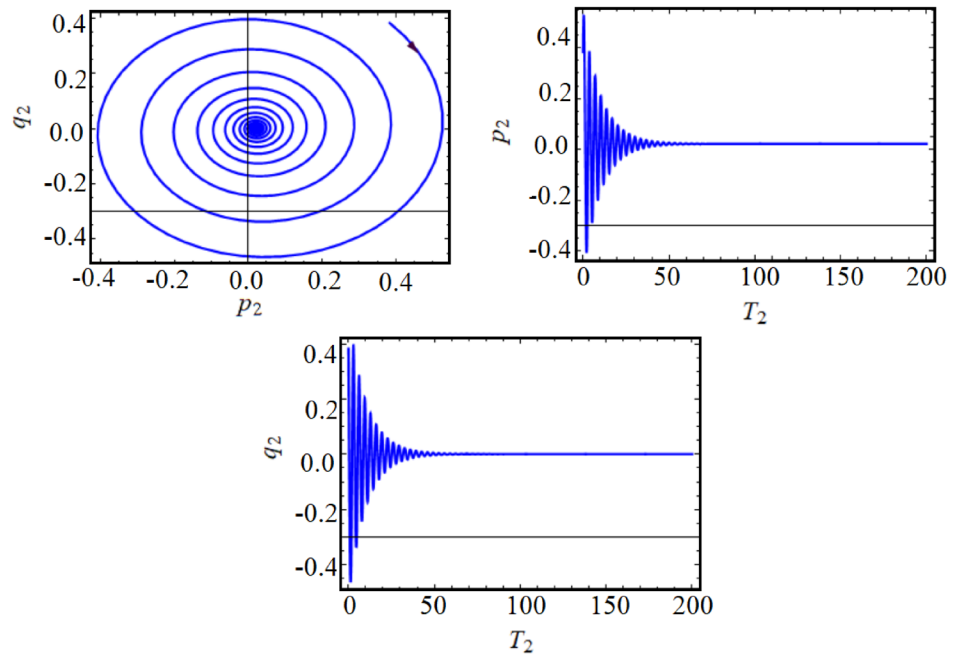


**Fig. 29** The modulation equation's projection on the plane  $p_2q_2$  and the adjusted amplitudes via time  $T_2$  when  $\sigma_2 = -0.005$ , and it is corresponding second fixed point in Fig. 21



the amplitude to some extent; see Fig. 3 and Fig. 4. Also, in Figs. 5, 6, 7, 8, 9, 10, when  $c_2$  and  $c_3$  increases, the number of oscillations of  $x$  and  $\theta$  decreases. The time history under the variation of  $\Omega_1$  is reported in Figs. 11, 12, 13 for the solutions  $r, x$ , and  $\theta$ , respectively, when time intervals  $T = [0 : 1000]$  and  $T = [0 : 100]$ . On the other side, we plot the time history for the solutions  $r, x$ , and  $\theta$  under the slight effect of  $\Omega_2$  as shown in Figs. 14, 15, 16.

It is obvious from Fig. 11 that the behavior of the attained waves for  $r$  varies between periodicity and decay and there is a slight effect for  $x$  and  $\theta$  as in Fig. 12 and Fig. 13. On the other side, we plot the time history for our solutions under the variation of  $\Omega_2$  in Figs. 14, 15, 16. According to the calculations depicted in these figures, when  $\Omega_2$  increases the amplitude of the waves of  $x$  decreases to reach to the decay behavior. Accordingly, we conclude that the motion of the system under consideration is stable and free of chaos.

## Non-linear Analysis

Our goal in this part is to show graphical representations of the analytical treatment developed in this paper for resonance situations of (28).

### Frequency–Response Curves

In Fig. 17, the modulation amplitudes of the three resonant modes are plotted via the parameter of detuning  $\sigma_3$  as a

control one to highlight the influence of some parameters on the system behavior up to the third-order of non-linearity. The physical dimensionless parameters have the next values

$$c_1 = 0.2, \quad c_2 = 0.2, \quad c_3 = 0.1, \quad f_1 = 0.1, \quad f_2 = 0.2, \quad f_3 = 0.3, \\ \Omega_1 = 0.65, \quad \Omega_2 = 1.2, \quad J = 1, \quad m = 0.5 \text{ kg}, \quad M^* = 1 \text{ kg}, \quad h = 0.1, \\ \epsilon = 0.001, \quad \mu = 0.5, \quad \sigma_1 = \sigma_2 = 0.$$

In the region,  $-10 < \sigma_3 < 10$  there exists one possible fixed point, in which it is stable in the range  $-0.8 < \sigma_3 \leq 10$  while it loses its stability as  $-10 < \sigma_3 < -0.8$ . Also Fig. 18 describes the modulation amplitudes under the impact of  $c_2$  when  $c_2 = 0.02$ . It is self-evident that, there is only one critical fixed point in which the stable and unstable fixed point exists in the domain  $4.8 < \sigma_3 < 10$  and  $-10 < \sigma_3 \leq 4.8$ , respectively. In Fig. 17, the detuning parameter  $\sigma_3$  takes the value  $-0.8$ , while in Fig. 18 has the value of  $4.8$ . The variation of  $c_3, \sigma_1$  and  $\sigma_2$  on the frequency response are explored in Figs. 19, 20, 21. The range of unstable and stable fixed points is drawn with a dashed line and a solid one, respectively. At certain instances, the system exhibits a transcritical bifurcation.

Now, we will provide the following transformation to explore the features of the equations of the system (35) for the non-linear amplitude. These equations will be modified by intruding the detuning parameter  $\sigma_k$  ( $k = 1, 2, 3$ ) to

examine the non-linear stability of this system. Therefore, the following convenient transformations are [35]

$$A_k = (p_k + iq_k)e^{i\sigma_k T_1},$$

where  $p_k$  and  $q_k$  are the real and imaginary parts of  $A_k$  respectively. We will have the following system:

The modified amplitudes were justified with the variation of time  $T_2$  in different parametric regions and the amplitudes' properties are graphed in the phase plane curves, as seen in Figs. 22, 23, 24, 25, 26, 27, 28, 29. In Fig. 22, the system has the same previous physical values of the parameters in Fig. 17. In Fig. 23, the same system is considered in Fig. (22), but with  $c_2 = 0.02$ . In Figs. 24, 25, The projection

$$\begin{aligned}
 & -2\Omega_1 p_1' + 2\Omega_1 \sigma_1 q_1 - \left[ \frac{3 - 2\Omega_1^2}{\Omega_1(\Omega_1 - 2)} + \frac{3 - 2\Omega_1^2}{\Omega_1(\Omega_1 + 2)} + \frac{(\Omega_1 - 1)^2}{\Omega_2^2 - (\Omega_1 - 1)^2} \right] \\
 & + 2(q_1 p_3^2 - q_1 q_3^2 + 2p_1 p_3 q_3) - c_1 \Omega_1 p_1 = 0, \\
 & -2\Omega_1 q_1' - 2\Omega_1 \sigma_1 p_1 + \left[ \frac{3 - 2\Omega_1^2}{\Omega_1(\Omega_1 - 2)} + \frac{3 - 2\Omega_1^2}{\Omega_1(\Omega_1 + 2)} + \frac{(\Omega_1 - 1)^2}{\Omega_2^2 - (\Omega_1 - 1)^2} - 2 \right] \\
 & (p_1 p_3^2 - p_1 q_3^2 - 2q_1 p_3 q_3) - c_1 \Omega_1 q_1 + \frac{1}{2} f_1 = 0, \\
 & -2\Omega_2 p_2' + 2\Omega_2 \sigma_2 q_2 - \frac{\Omega_2^4 J I}{(1 - \Omega_2^2)} q_2 - \frac{\mu \Omega_2^2}{\Omega_1^2 - (\Omega_2 + 1)^2} \times (2p_2 p_3 q_3 + q_2 p_3^2 \\
 & - q_2 q_3^2) - c_2 \Omega_2 p_2 = 0, \\
 & -2\Omega_2 q_2' - 2\Omega_2 \sigma_2 p_2 + \frac{\Omega_2^4 J I}{(1 - \Omega_2^2)} p_2 + \frac{\mu \Omega_2^2}{\Omega_1^2 - (\Omega_2 + 1)^2} (-2q_2 p_3 q_3 + p_2 p_3^2 \\
 & - p_2 q_3^2 - c_2 \Omega_2 q_2 + \frac{1}{2} f_2 = 0, \\
 & -2p_3' + 2\sigma_3 q_3 - \frac{3 - 2\Omega_1^2}{\Omega_1(2 + \Omega_1)} (2p_3 p_1 q_1 + q_3 p_1^2 - q_3 q_1^2) - c_3 p_3 - \frac{1}{\Omega_1^2} (q_3 p_3^2 - q_3^3 + 2p_3^2 q_3) \\
 & - 4\Omega_1^2 (2p_3 p_1 q_1 + q_3 p_1^2 - q_3 q_1^2) + \left[ \frac{\Omega_2^4}{\Omega_1^2 - (1 + \Omega_2)^2} + \frac{\Omega_2^4}{\Omega_1^2 - (1 - \Omega_2)^2} \right] \\
 & \times (2p_3 p_2 q_2 + q_3 p_2^2 - p_3 q_2^2) = 0, \\
 & -2q_3' - 2\sigma_3 p_3 + \frac{3 - 2\Omega_1^2}{\Omega_1(2 + \Omega_1)} (p_3 p_1^2 - p_3 q_1^2 - 2q_3 p_1 q_1) - c_3 q_3 + \frac{1}{\Omega_1^2} (p_3^3 - p_3 q_3^2 - 2q_3^2 p_3) \\
 & + 4\Omega_1^2 (p_3 p_1^2 - 2q_3 p_1 q_1 - p_3 q_1^2) - \left[ \frac{\Omega_2^4}{\Omega_1^2 - (1 + \Omega_2)^2} + \frac{\Omega_2^4}{\Omega_1^2 - (1 - \Omega_2)^2} \right] \\
 & \times (q_3 q_2^2 - p_3 p_2^2 - 2q_3 p_2 q_2) - \frac{1}{2} f_3 = 0.
 \end{aligned} \tag{41}$$

$p_2q_2$  plane and the corresponding modified amplitudes with  $c_3 = 0.001$  and it is corresponding to the fixed point in Fig. 19 in which  $\sigma_3$  takes the values,  $-2.9, -0.9$ , respectively. Also, Figs. 26, 27, 28, 29 show the projection  $p_2q_2$  plane and the corresponding modified amplitudes but in Figs. 26, 27 when  $\sigma_1$  has the value  $-1$  and these figures are corresponding to the first and the second fixed point in Fig. 20 in which  $\sigma_3$  equal  $-4.4$  and  $0.5$ . In Figs. 27, 28, when  $\sigma_2$  has the value  $-0.005$  and these figures are corresponding to the first and the second fixed point in Fig. 21 in which  $\sigma_3$  has the values  $-3.5, -0.4$ , respectively. These figures are clearly demonstrate that, the amplitudes diminish gradually with time and the density of the spiral cycle rapidly declines. This means that the system is stable under changing of parameters.

## Conclusion

The motion of the auto-parametric pendulum model with 3DOF consisting of a mass  $M$  attached to two massless springs with linear stiffness was investigated. Lagrange's equation is used to derive the controlling equations of motion. The approximate solutions and the resonance cases obtained using MMS. Criterion of Routh–Hurwitz is used to obtain the solvability condition at the steady state. The variations of the solutions via time are graphed to have the influence of some different parameters on the behavior of the dynamical model. The obtained results of higher consistency with the results in [11]. The characteristics of the non-linear amplitudes of the system are discussed to investigate its stability. The modulation amplitudes of the resonant modes are plotted via one of the detuning parameter as a control one to examine the impact of some parameters on the behavior of system. It is remarked that at certain values of this parameter, the system produces transcritical bifurcations. The solutions of modulation equations have stable fixed points, as shown from the solutions' projections on the plane  $p_2q_2$ . The achieved solutions are considered as a generalization of which are obtained in [29] for the case of rigid pendulum arm. The significance of the examined model can be seen in its applications in a variety of domains, including ship motion, transportation equipment, swaying buildings, and rotor dynamics.

**Acknowledgements** There was no specific grant for this research from any funding source in the public, private, or non-profit sectors.

**Funding** Open access funding provided by The Science, Technology & Innovation Funding Authority (STDF) in cooperation with The Egyptian Knowledge Bank (EKB).

**Data Availability** As no datasets were generated or processed during the current study, data sharing was not applicable to this paper.

## Declarations

**Conflict of Interest** There are no conflicts of interest declared by the authors.

**Open Access** This article is licensed under a Creative Commons Attribution 4.0 International License, which permits use, sharing, adaptation, distribution and reproduction in any medium or format, as long as you give appropriate credit to the original author(s) and the source, provide a link to the Creative Commons licence, and indicate if changes were made. The images or other third party material in this article are included in the article's Creative Commons licence, unless indicated otherwise in a credit line to the material. If material is not included in the article's Creative Commons licence and your intended use is not permitted by statutory regulation or exceeds the permitted use, you will need to obtain permission directly from the copyright holder. To view a copy of this licence, visit <http://creativecommons.org/licenses/by/4.0/>.

## References

- Ikeda T (2003) Nonlinear parametric vibrations of an elastic structure with a rectangular liquid tank. *Nonlinear Dyn* 33(1):43–70
- Cveticanin L, Zukovic M, Cveticanin D (2018) Oscillator with variable mass excited with non-ideal source. *Nonlinear Dyn* 92(2):673–682
- Yu TJ, Zhang W, Yang XD (2017) Global dynamics of an autoparametric beam structure. *Nonlinear Dyn* 88(2):1329–1343
- Cartmell M (1990) Introduction to linear, parametric, and nonlinear vibrations. Chapman and Hall, London
- Nayfeh AH, Mook DT (2008) Nonlinear oscillations. John Wiley & Sons, New Jersey
- Fossen T, Nijmeijer H (2011) Parametric resonance in dynamical systems. Springer Science and Business Media, Berlin
- Zhu S, Zheng Y, Fu Y (2004) Analysis of nonlinear dynamics of a two degree of freedom vibration system with nonlinear damping and nonlinear spring. *J Sound Vib* 271(1–2):15–24
- El Rifai K, Haller G, Bajaj AK (2007) Global dynamics of an autoparametric spring mass pendulum system. *Nonlinear Dyn* 49(1–2):105–116
- Kecik K, Warminski J (2011) Dynamics of an autoparametric pendulum like system with a nonlinear semiactive suspension. *Math Probl Eng*. <https://doi.org/10.1155/2011/451047>
- Kęcik K, Mitura A, Warmiński J (2013) Efficiency analysis of an autoparametric pendulum vibration absorber. *Eksploatacja i Niezawodność* 15(3):221–224
- Vazquez-Gonzalez B, Silva-Navarro G (2008) Evaluation of the autoparametric pendulum vibration absorber for a Duffing system. *Shock Vib* 15(3–4):355–368
- Khirallah K (2018) Autoparametric amplification of two nonlinear coupled mass spring systems. *Nonlinear Dyn* 92(2):463–477
- Nabergoj R, Tondl A, Virag Z (1994) Autoparametric resonance in an externally excited system. *Chaos Solitons Fract* 4(2):263–273
- Kamel M (2007) Bifurcation analysis of a nonlinear coupled pitch roll ship. *Math Comput Simul* 73(5):300–308
- Zhou L, Chen F (2008) Stability and bifurcation analysis for a model of a nonlinear coupled pitch–roll ship. *Math Comput Simul* 79(2):149–166
- Amer TS, Bek M (2009) Chaotic responses of a harmonically excited spring pendulum moving in circular path. *Nonlinear Anal Real World Appl* 10(5):3196–3202
- Bek MA, Amer TS, Sirwah AM, Jan A, Arab AA (2020) The vibrational motion of a spring pendulum in a fluid flow. *Results Phys* 19:103465

18. Moore H (2012) Matlab®, for engineers, 3rd edn. Pearson Education Inc, Upper Saddle River, pp 1–8
19. Amer T (2017) S, The dynamical behavior of a rigid body relative equilibrium position. *Adv Math Phys.* <https://doi.org/10.1155/2017/8070525>
20. Amer TS, Bek MA, Hamada IS (2016) On the motion of harmonically excited spring pendulum in elliptic path near resonances. *Adv Math Phys.* <https://doi.org/10.1155/2016/8734360>
21. Amer TS, Bek MA, Abouhmr MK (2018) On the vibrational analysis for the motion of a harmonically damped rigid body pendulum. *Nonlinear Dyn* 91(4):2485–2502
22. Meirovitch L (2001) *Fundamentals of vibrations.* McGraw-Hill Higher Education, New York
23. Nagashima I (2001) Optimal displacement feedback control law for active tuned mass damper. *Earthq Eng Struct Dyn* 30(8):1221–1242
24. Eissa M, Sayed M (2006) A comparison between active and passive vibration control of nonlinear simple pendulum, part II longitudinal tuned absorber and negative  $G\phi$  and  $G\phi_n$  feedback. *Math Comput Appl* 11(2):151–162
25. Eissa M, Sayed M (2008) Vibration reduction of a three DOF non-linear spring pendulum. *Comm Nonlinear Sci Numer Simulat* 13(2):465–488
26. El-Sabaa FM, Amer T, Gad HM, Bek MA (2020) On the motion of a damped rigid body near resonances under the influence of harmonically external force and moments. *Results Phys* 19:103352
27. Abady IM, Amer TS, Gad HM, Bek MA (2022) The asymptotic analysis and stability of 3DOF non-linear damped rigid body pendulum near resonance. *Ain Shams Eng J* 13(2):101554
28. Abohamer MK, Awrejcewicz J, Starosta R, Amer TS, Bek MA (2021) Influence of the motion of a spring pendulum on energy-harvesting devices. *Appl Sci* 11(18):8658
29. Amer WS, Amer TS, Starosta R, Bek MA (2021) Resonance in the cart-pendulum system-an asymptotic approach. *Appl Sci* 11(23):11567
30. He J-H, Amer TS, Abolila AF, Galal AA (2022) Stability of three degrees-of-freedom auto-parametric system. *Alex Eng J* 61(11):8393–8415
31. Amer TS, Bek MA, Hassan SS, Elbendary S (2021) The stability analysis for the motion of a nonlinear damped vibrating dynamical system with three-degrees-of-freedom. *Results Phys* 28:104561
32. Abdelhfeez SA, Amer TS, Elbaz RF, Bek MA (2022) Studying the influence of external torques on the dynamical motion and the stability of a 3DOF dynamic system. *Alex Eng J* 61(9):6695–6724
33. Bek MA, Amer TS, Almahalawy A, Elameer AS (2021) The asymptotic analysis for the motion of 3DOF dynamical system close to resonances. *Alex Eng J* 60(4):3539–3551
34. Amer TS, Bek MA, Hassan SS (2022) The dynamical analysis for the motion of a harmonically two degrees of freedom damped spring pendulum in an elliptic trajectory. *Alex Eng J* 61(2):1715–1733
35. Amer TS, Starosta R, Almahalawy A, Elameer AS (2022) The stability analysis of a vibrating auto-parametric dynamical system near resonance. *Appl Sci* 12:1737

**Publisher's Note** Springer Nature remains neutral with regard to jurisdictional claims in published maps and institutional affiliations.